MASTERARBEIT | MASTER'S THESIS

Titel | Title

(Radio)synthesis of sedoheptulose derivatives: first experiences

verfasst von | submitted by

Nikodemus Haberfellner BSc

angestrebter akademischer Grad | in partial fulfilment of the requirements for the degree of

Master of Science (MSc)

Wien | Vienna, 2024

Studienkennzahl lt. Studienblatt | Degree programme code as it appears on the student record sheet:	UA 066 862
Studienrichtung lt. Studienblatt | Degree programme as it appears on the student record sheet:	Masterstudium Chemie
Betreut von | Supervisor:	Univ.-Prof. Mag. Dr. Markus Mitterhauser
Mitbetreut von | Co-Supervisor:	Mag. Dr. Theresa Balber

Acknowledgments

First of all, I want to thank my supervisor Univ.-Prof. Mag. Dr. Markus Mitterhauser for giving me the opportunity to conduct my master thesis in the Joint Medicinal Applied Radiochemistry facility at the General Hospital of Vienna. Thank you for all the advice, guidance and motivating words during this work and for further sparking my fascination in radiochemistry.

Secondly, I want to thank my co-supervisor, Mag. Dr. Theresa Balber, who greatly supported me during my time in and outside the lab. Thank you for always taking your time with me and all the advice you provided during various progress reports, online-calls and lunch breaks.

A special thank you goes out to Kate, Julia and Lena, who made the weekly progress reports a meeting to look forward to.

Another special thank you goes out to Dr. Katharina Pallitsch, who allowed me to work on the reference compound in her lab at the Institute of Organic Chemistry during a maintenance period of the cyclotron. Thank you for always providing advice and the lovely time I had working in your laboratory.

Additionally, I want to thank the working group of Dr. Pallitsch, namely Tami, Sebi, Kristof and Naomi for the warm welcome in the group. I had a really lovely time during my stay at the group in and outside the lab.

Also, I want to thank my incredible parents for supporting me my whole life. It does not matter whether times are good or bad, you are always there.

Last but not least, I want to thank my girlfriend, Elena. No words can describe the amount of support and happiness you give me. Thank you, for being you.

Finally, I also want to take the opportunity to thank all people who have not been mentioned so far and were involved in my studies during my entire time at the University of Vienna.

Abstract

Background/Aim: Preliminary results of non-radiolabeled 4-desoxy-4-fluoro-D-sedoheptulose (4-FDS) have shown that the carbohydrate is internalized by human fibroblasts. After phosphorylation *via* sedoheptulose kinase (SHPK), the fluorine in the molecule should hinder further enzymatic degradation of the carbohydrate, which would make it an interesting radiopharmaceutical to apply the principle of metabolic trapping. The fluorinated sedoheptulose would allow insights into the role of rare carbohydrates in the pentose phosphate pathway in health and disease. The aim of this thesis is to prepare [^{18}F]fluoride labeled 4-deoxy-4-fluoro-D-sedoheptulose (4-FDS). A second aim is the development of a synthesis for a reference compound of 4-FDS bearing protecting groups.

Methods: The radioactive [^{18}F]fluoride was produced in a cyclotron *via* ^{18}O(p,n)^{18}F reaction. The [^{18}F]fluoride was trapped on an anion exchange cartridge and eluted with a solution of Kryptofix 2.2.2 and potassium carbonate. Residual water was removed via azeotropic distillation. The precursor 1,2,3,7-tetra-*O*-acetyl-5-*O*-benzoyl-4-*O*-trifluoromethanesulfonyl-D-glycero-α-D-lyxo-hept-2-ulopyranose was either dissolved in acetonitrile or *N,N*-dimethylformamide for small-scale radiolabeling test syntheses. After cartridge purification, reaction conditions towards the deprotection of the radiolabeled sedoheptulose were tested. A nine-step synthesis towards a reference compound of fluorinated and protected sedoheptulose was established. The precursor and a 4-FDS standard solution were used to develop a method for the characterization and analysis of the synthesized compounds.

Results: The fluorination of the precursor was feasible with conversion rates up to 20%. No full deprotection of radiolabeled sedoheptulose could be achieved. The synthesis of fluorinated and protected intermediate as a reference compound did not lead to the desired product.

Conclusions: [^{18}F]4-FDS could not be synthesized successfully *via* the approaches chosen so far. The radiosynthesis needs to be optimized to ensure reproducibility of the radiofluorination and achieve full deprotection. Quality control procedures for the products were established. The synthesis of the reference compound needs to be adapted, since the fluorination reactions were not feasible under the chosen reaction conditions.

Deutsche Zusammenfassung

Ziele: Versuchsergebnisse mit 4-Desoxy-4-fluoro-D-sedoheptulose (4-FDS) haben gezeigt, dass dieses Kohlenhydrat von menschlichen Fibroblasten in das Zytosol aufgenommen wird. Nach einer Phosphorylierung durch das Enzym Sedoheptulosekinase (SHPK), ist der weitere enzymatische Abbau durch das Fluoratom im Kohlenhydrat nicht möglich. Dies würde 4-FDS zu einem interessanten Radiopharmazeutikum machen, um das Prinzip des „Metabolic Trapping“ anzuwenden. 4-FDS könnte Einblicke in die Rolle dieses Zuckers im Kohlenhydratstoffwechsels, insbesondere im Pentosephosphatweg, ermöglichen. Das Ziel dieser Arbeit ist die Synthese 4-[^{18}F]-FDS. Ein weiteres Ziel ist die Erstellung einer Synthese einer Referenzverbindung von 4-FDS mit Schutzgruppen.

Methoden: Das radioaktive [^{18}F]Fluoridion wurde in einem Zyklotron durch eine ^{18}O(p,n)^{18}F Kernreaktion erzeugt. Das [^{18}F]Fluoridion wurde auf einer Anionenaustauscherkartusche adsorbiert und mitttels einer Lösung aus Kryptofix 2.2.2 und Kaliumcarbonat eluiert. Das Restwasser wurde durch azeotrope Destillation entfernt. Für Testmarkierungsversuche wurde der Precursor 1,2,3,7-tetra-*O*-acetyl-5-*O*-benzoyl-4-*O*-trifluormethansulfonyl-D-glycero-α-D-lyxo-hept-2-ulopyranose wurde in Acetonitril oder *N,N*-Dimethylformamid gelöst. Nach einem Aufreinigungsschritt, wurden mögliche Reaktionsbedingungen für die Entschützung von 4-[^{18}F]FDS getestet. Zusätzlich wurde eine mehrstufige Synthese für eine Referenzverbindung der fluorierten und geschützten Sedoheptulose etabliert. Es wurde mittels Precursor und der 4-FDS Standardlösung eine Methode zur Charakterisierung der synthetisierten Verbindungen entwickelt.

Ergebnisse: Bei der Radiofluorierung konnten Umsätze von bis zu 20 % erreicht werden. Eine vollständige Entschützung der radiomarkierten Sedoheptulose war unter den getesteten Reaktionsbedingungen nicht möglich. Die mehrstufige Synthese für die fluorierte und geschützte Sedoheptulose als Referenzverbindung führte nicht zum gewünschten Produkt.

Schlussfolgerungen: [^{18}F]4-FDS konnte bisher noch nicht erfolgreich synthetisiert werden. Die Bedingungen der Radiosynthese müssen noch optimiert werden, um höhere Umsätze zu erzielen und Reproduzierbarkeit zu gewährleisten. Zusätzlich müssen die Entschützungsbedingungen überarbeitet werden, um eine vollständige Entschützung zu erreichen. Erste Qualitätskontrollverfahren für die Syntheseprodukte wurden erstellt. Die Synthese der fluorierten und geschützten Referenzverbindung muss adaptiert werden, da die Fluorierungsreaktionen nicht zu dem gewünschten Reaktionsprodukt führten.

Table of contents

Theoretical background

Fluorination reactions

Due to their unique properties, fluorinated molecules have become increasingly important in the pharmaceutical, agrochemical and medicinal industry over the last decades.[1] The introduction of fluorine atoms in organic compounds can significantly alter their chemical and physiological properties compared to their naturally occurring counterparts. The effect ranges from different lipophilicity, metabolic stability and steric conformation to altered basicity and hydrogen bonding.[2] Due to the similarities in bond length and polarization between C-F and C-OH, fluorine poses an ideal element to synthesize bioisosteres of naturally occurring carbohydrates for biochemical investigations.[3,4] While only a few naturally occurring fluorinated compounds are known, the prevalence of fluorinated drugs approved by the FDA has steadily risen over the last years.[5] The synthetic and radioactive isotope fluorine-18 can be used to tag biochemical probes for the study of a variety of biological processes. More importantly, fluorine-18 is used daily in positron-emission tomography (PET) for diagnosing and detecting a wide range of diseases including cancer.[1] Due to the various applications of fluorinated compounds, the development of synthetic strategies for the introduction of C-F bonds into organic molecules is of great importance and extensively studied. Fluorination reactions can be divided into nucleophilic and electrophilic fluorination reactions.

Although the fluoride ion is a strong nucleophile it forms hydrogen bonds in aqueous solutions, which significantly decreases the reactivity. To avoid the decrease in reactivity it is necessary to remove any water from the reaction mixture. Subsequent substitution reactions are mostly conducted in polar aprotic organic solvents like acetonitrile (ACN), *N,N*-dimethylformamide (DMF) or dimethyl sulfoxide (DMSO) under elevated temperatures. To enhance the solubility and reactivity of fluoride ions in organic solvents the use of phase transfer catalysts (PTC) – such as Kryptofix 2.2.2 – are employed.[6] An alternative route to enhance solubility and reactivity is the addition of bulky tetrabutylammonium cations.[7] In radiochemical approaches the nucleophilic fluorinations are typically conducted in the presence of poorly nucleophilic bases (mostly carbonate and bicarbonate ions) and residual water is removed by an azeotropic distillation assisted by acetonitrile.[8]

Once the process of drying is complete, the fluoride ion can be introduced into an aliphatic position *via* a S_N2 substitution reaction as shown in Figure 1.

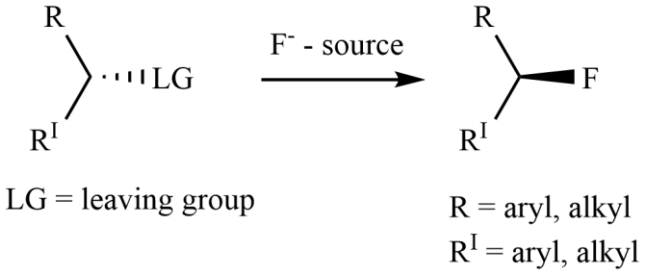

Figure 1: Nucleophilic S_N2-type fluorination reaction. The reaction proceeds with an inversion of stereochemistry. R= alkyl, aryl; R^I = alkyl, aryl.

The precursors used for these reactions typically contain a leaving group, such as a triflate group. A critical step in the design of fluorination reactions is the selection of the best leaving group. It should be stable under the chosen reaction conditions and should prevent undesired side reactions, such as the competing elimination reaction.[7] Nevertheless, a fast and quantitative cleavage should be possible under the chosen reaction conditions. Since S_N2 substitutions mostly proceed via an inversion of the configuration, it is important to retain the native ligand conformation in the products to avoid negative effects on their binding affinities.[5]

In electrophilic substitution reactions, the electrophile is a reagent delivering an "F^+" ion and the nucleophile is an electron-rich reagent. The nucleophile can be a carbanion (e.g. Grignard-reagent), an unsaturated compound (alkene, alkyne or aromatic) or a substrate bearing a nucleophilic and labile bond (e.g. C-Si or C-B).[1] The high reactivity and lability pose the biggest drawback of electrophilic fluorine sources and limit their applications and the development of synthetic strategies significantly. A breakthrough in electrophilic fluorination reactions is the development of bench-stable reagents bearing an N-F bond.[1] Two key representatives of this reagent class are shown in Figure 2.

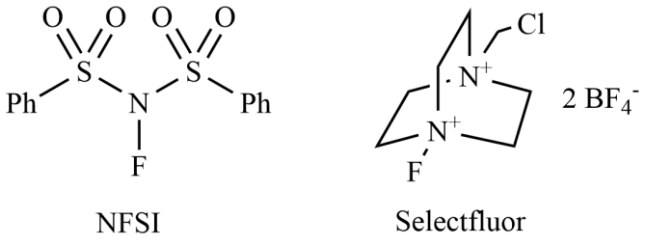

Figure 2: Examples of electrophilic fluorine sources bearing an N-F bond. NFSI=N-fluorobenzenesulfonimide. Selectfluor=1-chloromethyl-4-fluoro-1,4-diazoniabicyclo[2.2.2]octane bis(tetrafluoroborate)

With these compounds it is possible to circumvent stability issues of previous "F^+" ion sources and enhance the yields of electrophilic fluorination reactions.

Radiofluorination of [^{18}F]FDG and clinical applications

One of the most important fluorination reactions in clinics is the synthesis of the diagnostic radiotracer 2-desoxy-2-fluoro-D-glucose ([^{18}F]FDG), which is often considered the "working horse" of nuclear medicine.[9] [^{18}F]FDG is used as a tracer for visualizing glucose metabolism *in vivo*. The fluorination is performed with the synthetic and radioactive isotope fluorine-18.

Fluorine-18 has a half-life of 110 minutes, a "clean" decay (97% β^+ -Emission) and positron energy (635 keV). It is one of the most frequently used radionuclides in positron emission tomography (PET).[10] Fluorine-18 is produced in a cyclotron. It can either be produced *via* ^{20}Ne(d,α)^{18}F reaction for electrophilic radiofluorinations, or *via* ^{18}O(p,n)^{18}F reaction for nucleophilic fluorinations. Fluorine-18 has countless applications for studies in oncology, cardiology and neurology.[11]

In early approaches, the radiopharmaceutical was produced *via* electrophilic fluorination through the addition of trifluoromethyl hypofluorite, elemental fluorine, xenon difluoride or acetylhypofluorite to the precursor tri-O-acetyl-D-glucal.[11,12] Today, the more commonly used reaction to obtain this compound, is a nucleophilic substitution on a peracetylated mannose-triflate precursor by a radioactive [^{18}F]fluoride ion using Kryptofix 2.2.2 as a PTC.

In radiosynthesis the deprotection needs to be fast, and employ conditions, where the tracer molecule stays intact. Through fast and quantitative reactions, acceptable radiochemical yields (RCY) of the final products are achieved.

After the substitution reaction the protecting groups are cleaved under acidic or basic conditions at room temperature yielding [^{18}F]FDG (Figure 3).[13]

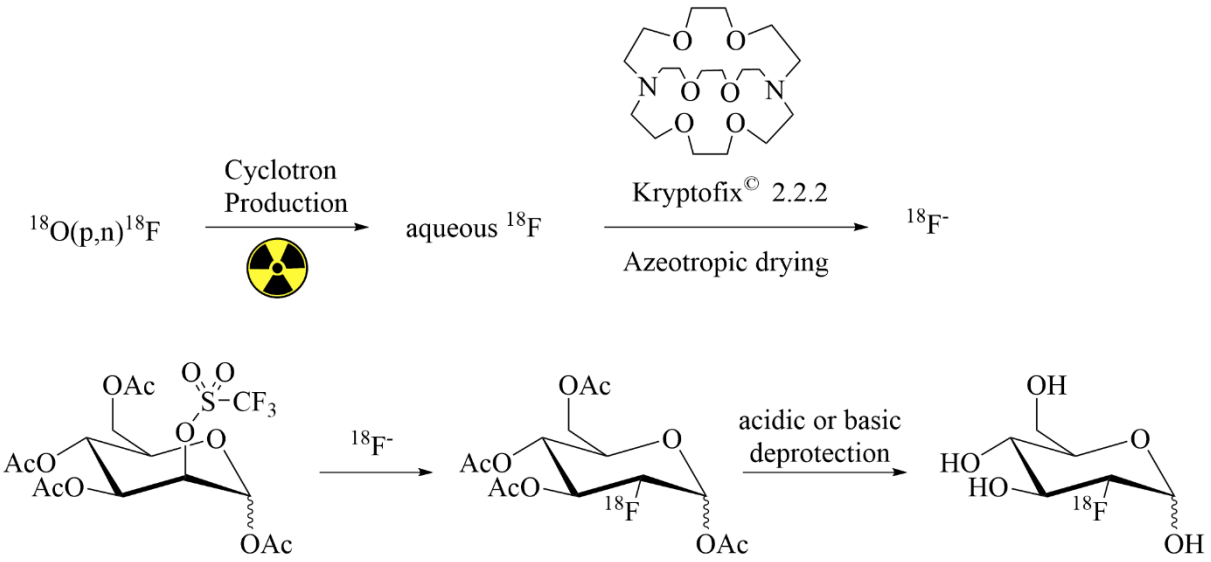

Figure 3: Synthesis of [^{18}F]FDG by nucleophilic substitution

Before its administration to patients, the tracer undergoes extensive quality control protocols.[13] Since the quality control needs to be performed right after synthesis, it is necessary that quality control takes a minimum amount of time. Therefore, improving the quality control processes is still important in research.[14]

One of the biggest drawbacks of [^{18}F]FDG is the high glucose demand of the brain, which can make the visualization of cancerous tumours in the brain impossible. Additionally, fluorine-18 is no naturally occurring isotope of fluorine. Therefore, a cyclotron is needed to produce the synthetic isotope.

Radionuclides in Medicine

Production of radionuclides

Radionuclides are radioactive nuclides which are used in medicine for diagnostic and therapeutic applications. Radionuclides decay according to their respective half-lives. Most naturally occurring radionuclides have very long half-lives, often thousands of years. Such long half-lives are not suitable for diagnostic or therapeutic purposes of nuclear medicine since most of the administered radiation dose is attributed to the patient outside the window for imaging or therapy. Therefore, the need to produce short lived radionuclides in medicine is high. For this purpose, four main methods of radionuclide production were implemented: fission, neutron activation, cyclotron production and generator elution.[15] Since the first two methods require a nuclear reactor, they will not be further discussed in this thesis.

Generator production of radionuclides

A radionuclide generator provides on-site availability of short-lived radionuclides. The generator contains a column or resin and a parent/daughter radionuclide pair. The short-lived daughter nuclide is eluted from the generator. The parent nuclide restores the daughter nuclide *via* radioactive decay. The separation of the parent/daughter radionuclide is usually based on chemical or physical properties. The most widely used generator in nuclear medicine is the $^{99}Mo/^{99m}Tc$ generator.[15]

Cyclotron production of radionuclides

Cyclotrons bombard stable nuclei with high energy, charged alpha particles like protons (p), deuterons (d), triton (t) or even helium nuclei. The cyclotron consists of semicircular electrodes in a vacuum within a magnetic field. Charged particles (mostly hydride ions H^-) which need to be accelerated are placed in the middle of the cyclotron and a high voltage is applied to the electrodes using a high frequency oscillator. The charged particles are accelerated through attraction to opposite charges, which are induced through the oscillator. The magnetic field ensures that the particles travel within the spiral. Once the desired energy of the particles is reached, the charged particles are passed through a thin foil of graphite to strip the electrons from the negatively charged ions to produce protons.[16] The protons are then directed towards the target. This bombardment causes nuclear transformation and produces the desired radionuclides. Table 1 shows some of the more common cyclotron reactions used to produce radionuclides and their respective half-lives [17]:

Table 1: Half-life and nuclear reaction of selected radionuclides generated with a cyclotron. p: proton, n: neutron, α: ^4_2He.

radionuclide	half-life $t_{1/2}$	nuclear reaction
^{11}C	20 min	$^{14}N(p,\alpha)^{11}C$
^{13}N	10 min	$^{16}O(p,\alpha)^{13}N$
^{18}F	110 min	$^{18}O(p,n)^{18}F$
^{64}Cu	12.7 h	$^{64}Ni(p,n)^{64}Cu$
^{67}Ga	3.26 d	$^{68}Zn(2p,n)^{67}Ga$

Due to their short half-lives, the radionuclides carbon-11 and nitrogen- 13 need to be produced directly before a planned radiosynthesis. The other radionuclides can also be shipped from facilities, which produce radionuclides, to sites of radiosynthesis (e.g. hospitals).

Positron Emission Tomography (PET)

Positron-Emission Tomography (PET) is one of the most sensitive non-invasive imaging techniques in the clinics. PET scans are used to visualize metabolic activity, blood flow and other physiological processes. Therefore, it is used to confirm cancer diagnoses or to plan further medical treatment in personalized medicine.[18] PET takes advantage of highly selective tracer molecules, which are linked to short-lived radionuclides such as fluorine-18, carbon-11, and gallium-68. These radioisotopes constantly decay by positron emission (β^+-decay). The emitted positron, which is the antiparticle of an electron, can travel a few millimeters (known as positron range) in human tissues until it collides with an electron.[19] They annihilate and during this event two high-energy annihilation photons are emitted at a 180° angle [20] (Figure 4).

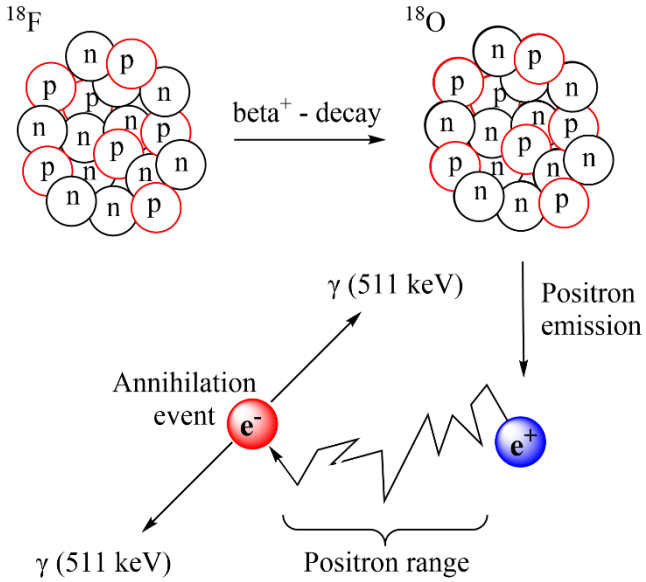

Figure 4: Principle of β^+-decay. ^{18}F decays via positron emission to ^{18}O. The positron (blue) travels until it reaches an electron (red), and an annihilation event occurs. Subsequently, two photons with an energy of 511 keV are emitted at a 180° angle. (n = neutron; p = proton)

The positron range is influenced by the energy of the positron and the type of radionuclide. With increasing positron range the spatial resolution of a PET scan gets poorer. The photons are detected by a surrounding gamma-detector array along the line of response (LOR). Through constant decay, numerous annihilation events are detected, which makes a localization of the annihilation events possible.[18] Spatial reconstruction of the annihilation events via data processing leads to the final PET image in three dimensions (Figure 5).

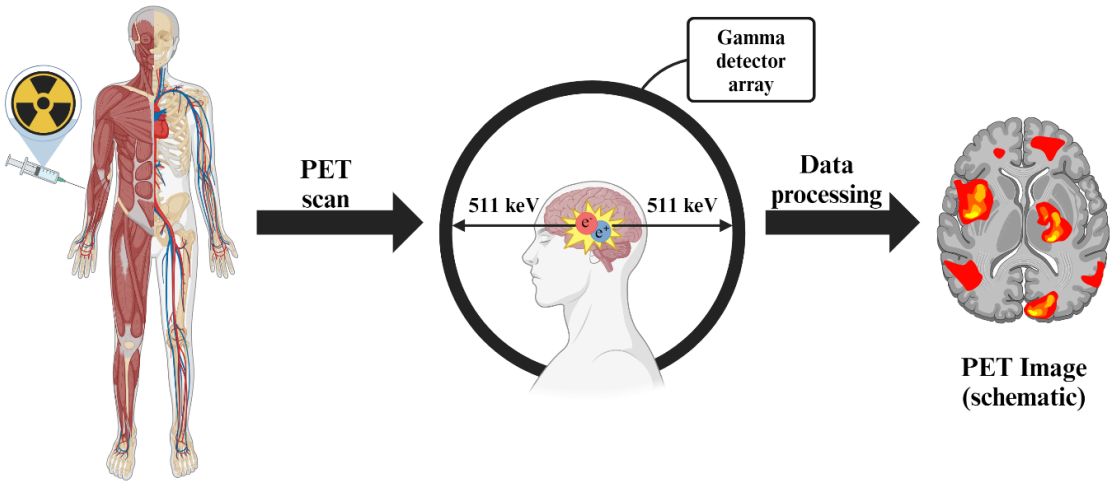

Figure 5: Principle of a PET scan. First a radiopharmaceutical is administered to the patient. After distribution in the body the annihilation photons are detected along the LOR (line of response, indicated by small black arrows) by a gamma detector array. Computer-assisted data processing leads to the final image.

PET radionuclides can be attached to imaging probes via different reactions. They can be covalently bound to small organic molecules or chelated.

The role of fluorinated carbohydrates in PET

Radiofluorinated carbohydrates have been of great interest in nuclear medicine since the discovery of [^{18}F]FDG.[21] The strategic incorporation of [^{18}F]fluoride into carbohydrate scaffolds made studies of a variety of metabolic processes possible. Over the last decades many fluorinated carbohydrate derivatives have been synthesized. Figure 6 shows some examples of fluorinated carbohydrates used for imaging of infections and metabolic processes.

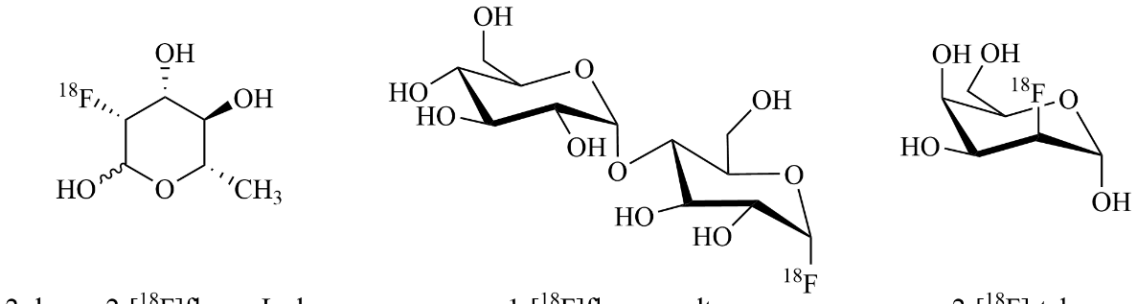

2-deoxy-2-[^{18}F]fluoro-L-rhamnose 1-[^{18}F]fluoro-maltose 2-[^{18}F]-talose

Figure 6: Examples of carbohydrate-based PET tracers used in research

Fluorine-18-labeled L-rhamnose derivatives have been synthesized as potential PET tracers for infections caused by fungal and bacterial strains.[22] *In vitro* experiments in *E. coli* using fluorinated maltose derivatives have shown promising results for detection and monitoring of

infections caused by bacteria [23]. Haradihara *et al*. reported a fluorine-18 labelled analogue of D-Talose for the study of galactose metabolism and liver function [24].

Recent advances in research also employed enzymatically catalysed reactions for introducing fluorine-18 into the carbohydrate scaffold [25].

Carbohydrates and their role in metabolic pathways

General

Carbohydrates are one of the most abundant groups of biomolecules on earth and represent the basic building blocks of plant structures. This group of molecules is the main source of energy for animals and humans alike and is used for the synthesis of glycoproteins and glycolipids as well as a general precursor for other complex biomolecules in the human body.[26] Interactions between carbohydrates and proteins (such as enzymes) play a pivotal role in a variety of biological processes related to health, reproduction and disease.[27] In nature, they are mainly produced by plants through photosynthesis. This process involves the fixation of carbon dioxide from the atmosphere finally yielding mono-, di-, oligo- and polysaccharides as well as oxygen. Di- and polysaccharides consist of saccharide monomers linked by glycosidic bonds.[28] The structural diversity in polysaccharides is enormous due to the variety of monosaccharides and the manifold of possible connections.

Glycolysis

Carbohydrate metabolism is a highly complex process. In the last decades, the involved processes have been extensively studied since carbohydrates play a key role in many physiological functions. They serve as an energy source in catabolic processes generating adenosine-triphosphate (ATP) or can be used in anabolic processes, such as the biosynthesis of fatty acids.[29] Carbohydrates can also be used by the body as an energy storage in the form of glycogen, which via gluconeogenesis is converted to glucose again to maintain blood sugar homeostasis. As glycolipids, sugars play an important role as components of cell membranes.[30] Sugars in the form of glycoproteins also exhibit effects in cellular signaling processes.[31]

Monosaccharides, such as glucose, fructose or galactose can directly enter glycolysis to meet the metabolic demands of a cell. The fate of these sugars can be quite diverse because they all enter carbohydrate metabolism through different pathways and at different points as illustrated in Figure 7.[29]

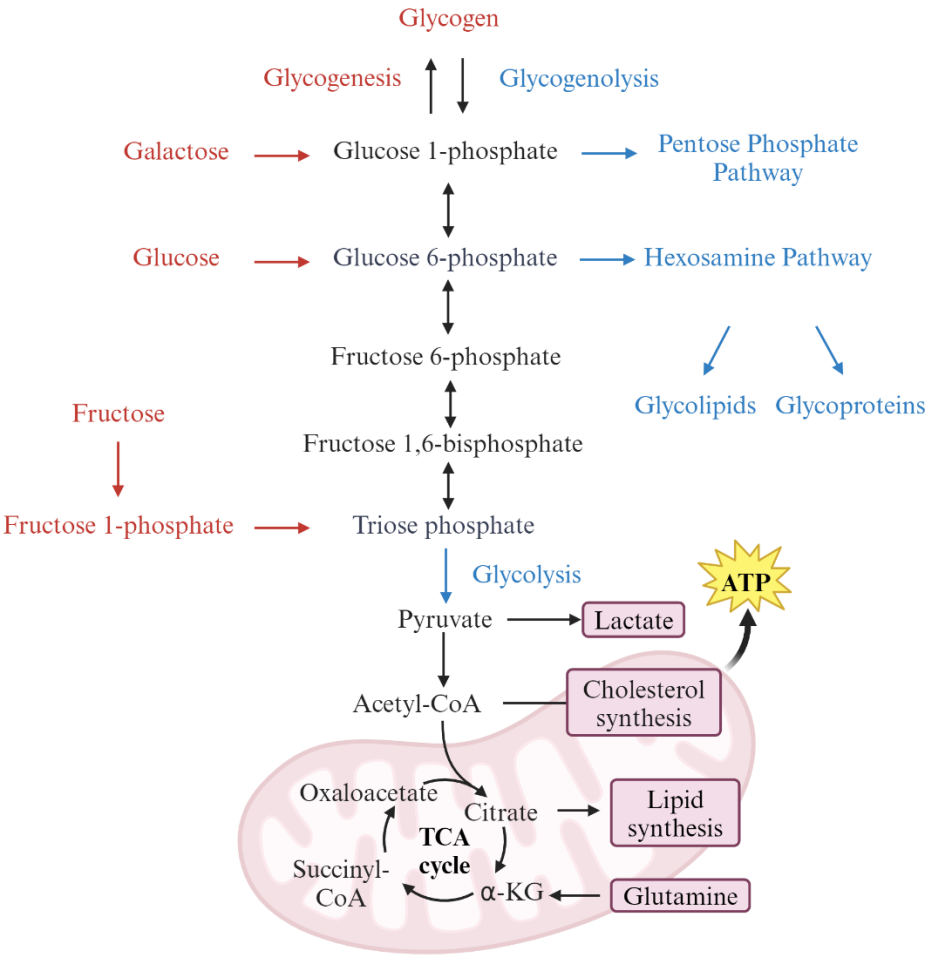

Figure 7: Overview of carbohydrate metabolism of glucose, fructose and galactose. [created with Biorender.com]

Glucose is taken up by cells through GLUT transporters. Then it enters glycolysis after an ATP-dependent phosphorylation by enzymes called hexokinases (HK).[32] Galactose catabolism occurs through the Leloir pathway in which a galactose molecule is phosphorylated via galactokinase to give galactose-1-phosphate. Galactose-1-phosphate subsequently gets metabolized to glucose-6-phosphate via transferase and phosphoglucomutase enzymes.[33] In highly proliferating cells, such as cancer cells, the glucose-6-phosphate generated from galactose preferentially enters the pentose phosphate pathway (PPP). This is caused by the high demand of ATP and ribose-5-phosphate in rapidly growing cells, which cannot be met by glycolysis alone and would lead to cell death.[29]

Fructose is metabolized through phosphorylation by fructokinase to give fructose-1-phosphate (F1P). Following phosphorylation, F1P is then cleaved into glyceraldehyde and dihydroxyacetone phosphate (DHAP) by a specific aldolase. The formed glyceraldehyde is then phosphorylated by triose kinase and the two triose intermediates can then be shuffled back into glycolysis.[34]

Pentose Phosphate Pathway (PPP)

The pentose phosphate pathway (PPP), also known as the hexose monophosphate shunt or the phosphogluconate pathway is a fundamental component of cellular metabolism.[35] It plays a key role in maintaining carbon homeostasis, providing precursors for nucleotide and amino acid biosynthesis and fighting oxidative stress in cells.[36] Also, the PPP is one of the major sources of nicotinamide adenine dinucleotide phosphate (NADPH) which plays a key role in fatty acid biosynthesis and the scavenging of reactive oxygen species (ROS). NADPH is critical for maintaining the redox balance in stress situations when cells proliferate quickly.[37] Due to this fact, the PPP plays a key role for cancer cells in maintaining their anabolic demands and combating oxidative stress.[35]

The PPP is divided into an oxidative and a non-oxidative branch. The oxidative branch is highly active in most eukaryotic organisms and converts glucose-6-phosphate (G6P) into carbon dioxide, ribulose-5 phosphate (Ru5P) and two equivalents of NADPH.[38] The non-oxidative branch converts fructose-6 phosphate (F6P) and glyceralydehyde-3 phosphate (GA3P) – both intermediates derived from glycolysis – as well as sedoheptulose-7-phosphate sugars to ribose-5 phosphate (R5P) a precursor for nucleotide biosynthesis.[39] The oxidative branch of the PPP is considered unidirectional since it comprises two irreversible steps. The non-oxidative branch is a highly dynamic system and consists of a series of reversible reactions involving different sugar phosphates. Two important enzymes of the non-oxidative PPP are transaldolase (TALDO1) and transketolase (TKT).

The regulation of the PPP has been of great interest in research in the last years.[39] An observation of the up- and downregulation of this pathway can lead to new insights on how the body deals with external and internal stress situations.[40]

As illustrated in Figure 8, the pathways of carbohydrate metabolism are strongly connected to each other and are influenced by many factors. The complex interplay between these pathways can be studied in health and disease by using different carbohydrate-based tracers. Thus, the synthesis and design of imaging probes to visualize carbohydrate metabolism *in vivo* is of high scientific interest.[19]

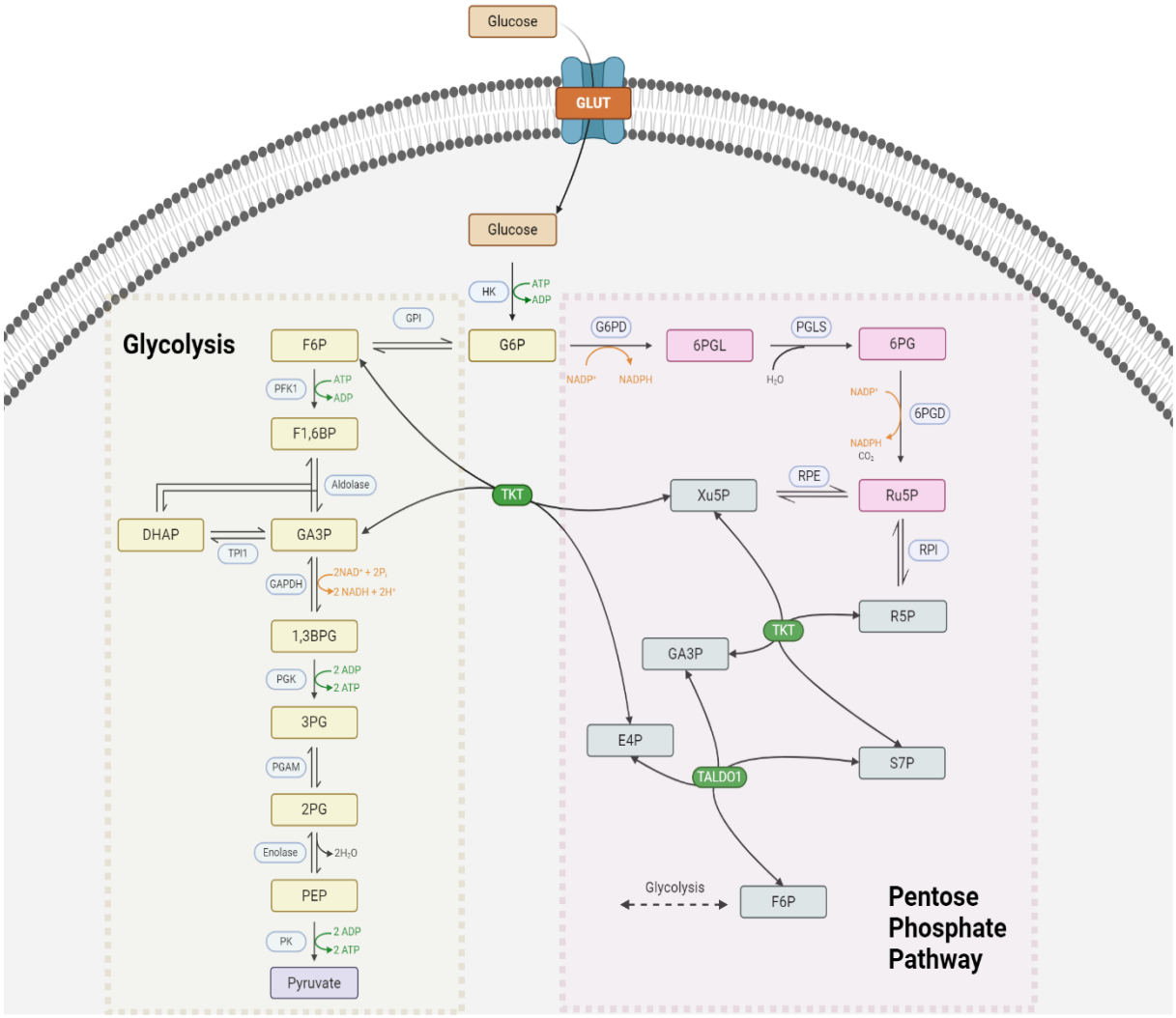

Figure 8: Overview and interactions between glycolysis and the PPP. [created with Biorender.com]

Figure 8 provides an overview of glycolysis, the PPP and their interactions. The key intermediates shared by both metabolic pathways are: F6P, glyceraldehyde-3 phosphate (GA3P), xylulose-5 phosphate (Xu5P) and erythrose-4 phosphate (E4P). The human body can react to the metabolic demands of a cell quickly and shift the equilibria of the non-oxidative branch towards the needed metabolites.[29,40]

The rare carbohydrate sedoheptulose

Sedoheptulose is a naturally existing ketose with a carbon scaffold consisting of seven carbons (Figure 9).[41] As a so called "rare carbohydrate" it has a significantly lower abundance in nature. Due to the low amounts of "rare carbohydrates" in natural sources, the extraction of this sugars is either not feasible or very challenging.[42]

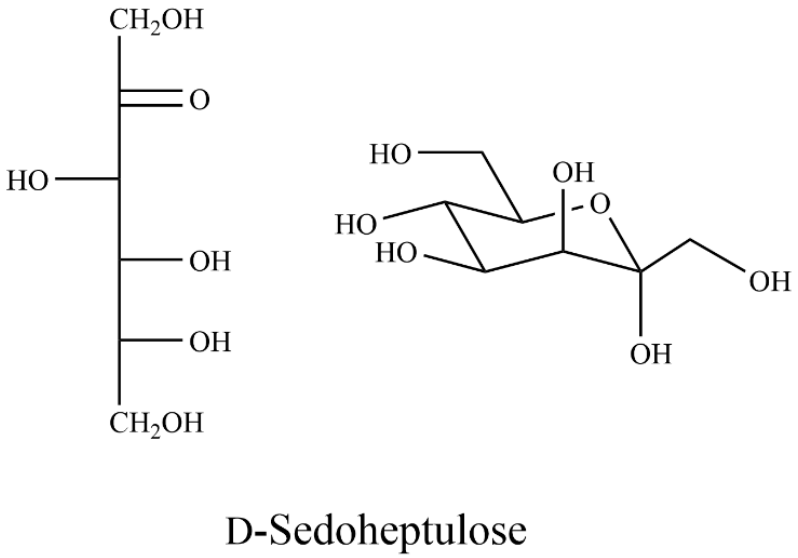

Figure 9: Structure of D-sedoheptulose in Fischer-projection and pyranose chair form.

In its phosphorylated form, it is a metabolite in the pentose phosphate pathway (see chapter "PPP") and plays an important role in carbohydrate metabolism in the body.[43] Nagy and Haschemi have shown that sedoheptulose can be directly phosphorylated via a specific kinase, namely sedoheptulose kinase (SHPK). They introduced SHPK as a rate-limiting enzyme in primary carbohydrate metabolism and showed the importance of this enzyme for balancing redox processes, cellular glucose consumption and nucleotide precursor formation.[41]

Principles of Metabolic trapping and rationale for the presented work

The term "metabolic trapping" refers to a principle in radiopharmaceutical drug design which was first introduced by Gallagher and coworkers in 1978.[44] It means that a radiopharmaceutical is taken up by cells and enzymatically converted into a metabolic product which cannot be further metabolized and therefore accumulates inside key tissues in the human body [45].

The best example to illustrate this principle is the radiotracer [^{18}F]FDG. The tracer is taken up by cells via GLUTs and subsequently phosphorylated by hexokinases (HK), which is the first step of glycolysis. The resulting [^{18}F]FDG-6 phosphate ([^{18}F]FDG6P) is not accepted as a substrate by the enzyme glucose phosphate isomerase (GPI) and cannot be further metabolized (Figure 10).[44]

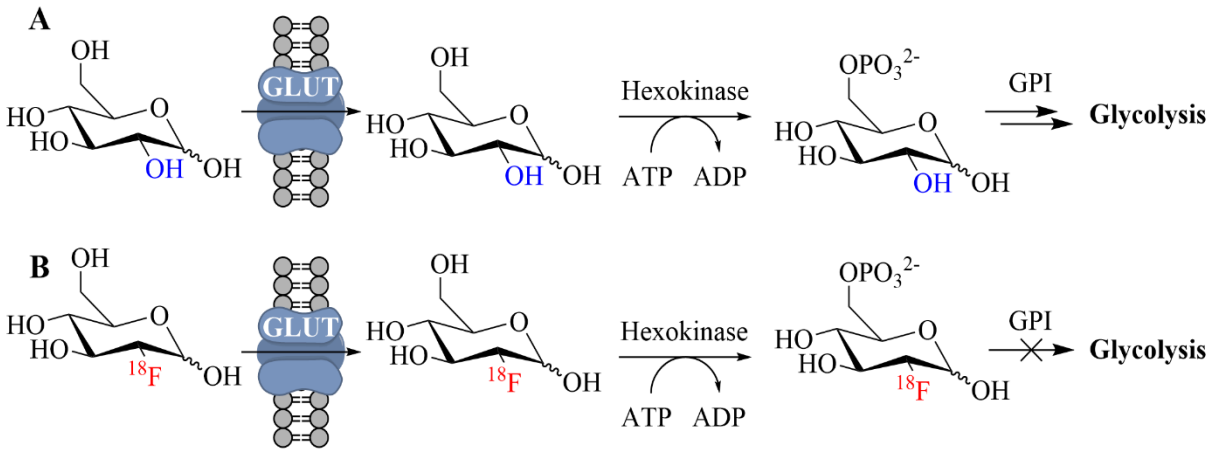

Figure 10: Comparison of glucose and [^{18}F]FDG metabolism leading to "metabolic trapping " of [^{18}F]FDG-6 phosphate in key tissues. ***A:*** *Glucose is taken up by GLUTs into the cytosol. HK phosphorylates glucose yielding glucose-6 phosphate (G6P). GPI isomerizes G6P to fructose-6 phosphate as the next step in glycoysis.* ***B:*** *[^{18}F]FDG is taken up by GLUTs and phosphorylated via HK yielding [^{18}F]FDG6P. GPI does not accept [^{18}F]FDG6P as a substrate and is not further metabolized.*

This causes the metabolite [^{18}F]FDG6P to accumulate inside key tissues. Cells with an altered or heightened carbohydrate metabolism (such as tumor cells) can be visualized using this principle.[44]

In preliminary biochemical studies, Scheibelberger *et al.* have shown that 4-deoxy-4-fluoro-D-sedoheptulose (4-FDS) is taken up by human fibroblasts and phosphorylated by sedoheptulose kinase (SHPK). Furthermore, the authors showed that the phosphorylated and fluorinated sedoheptulose is not accepted as a substrate by the enzymes TALDO1 or TKT. This data indicates a metabolic trapping mechanism similar to that of FDG. Therefore, we hypothesize that radiolabeled sedoheptulose derivatives could be useful tools to provide further insights into the highly complex carbohydrate metabolism in health and disease.

A synthetic route for a potential radiolabeling precursor of [^{18}F]4-FDS was established by the working group of Dr. Katharina Pallitsch. The final synthesis is summarized in Figure 11.[46]

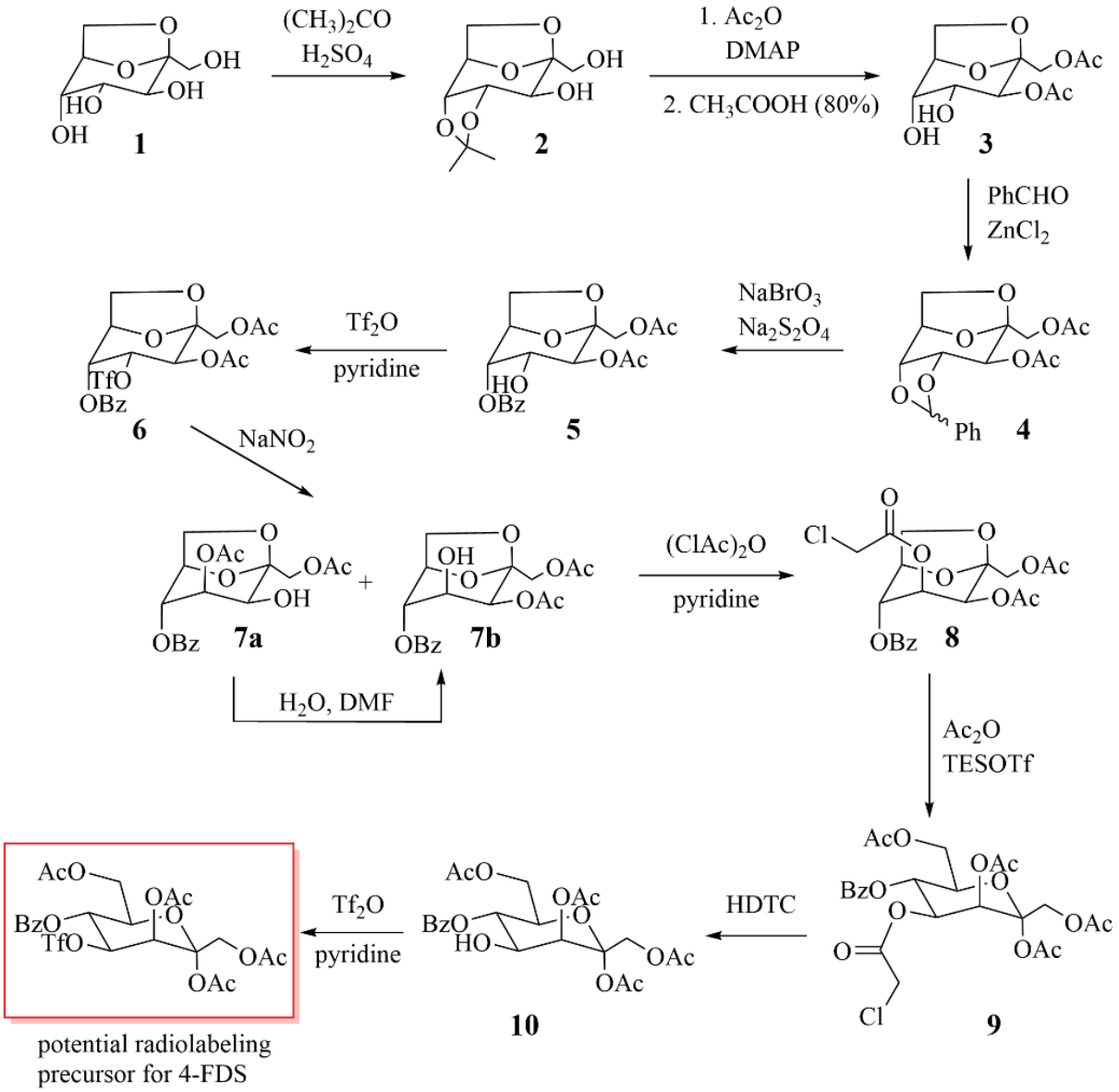

Figure 11: Synthetic scheme towards the radiolabeling precursor 1,2,3,7-tetra-O-acetyl-5-O-benzoyl-4-O-trifluoromethanesulfonyl-D-glycero-alpha-D-lyxo-hept-2-ulopyranose as published by Scheibelberger et al.

Hypothesis and Aim of the thesis

The discovery of sedoheptulose kinase (SHPK) indicates that sedoheptulose can directly enter the pentose phosphate pathway (PPP).[41] It was recently shown that the incorporation of the fluorine atom at position 4 of the carbohydrate scaffold hinders enzymatic degradation of sedoheptulose-7 phosphate in cells.[46] Therefore, we hypothesize that fluorinated sedoheptulose would be a useful tool to perform cell studies, biodistribution studies and elucidate the regulatory mechanisms of the PPP thereby allowing further insights into the highly complex carbohydrate metabolism in health and disease.

The first aim of this thesis is to establish a procedure for reproducible radiolabeling of the precursor 1,2,3,7-tetra-*O*-acetyl-5-*O*-benzoyl-4-*O*-trifluoromethanesulfonyl-D-glycero-α-D-lyxo-hept-2-ulopyranose with [^{18}F]fluoride yielding 1,2,3,7-tetra-*O*-acetyl-5-*O*-benzoyl-4-[^{18}F]fluoro-D-glycero-α-D-lyxo-hept-2-ulopyranose (Figure 12). The precursor is provided by Dr. Katharina Pallitsch. and is designed for the late stage incorporation of [^{18}F]fluoride.

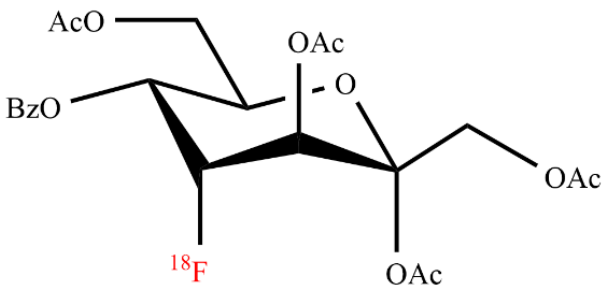

Figure 12: Structure of 1,2,3,7-tetra-O-acetyl-5-O-benzoyl-4-[^{18}F]fluoro-D-glycero-α-D-lyxo-hept-2-ulopyranose in pyranose chair conformation

The second aim of this thesis is to establish a procedure for total and fast deprotection after successful radiofluorination. This would yield the desired radiofluorinated product 4-deoxy-4-[^{18}F]-fluorosedoheptulose (Figure 13).

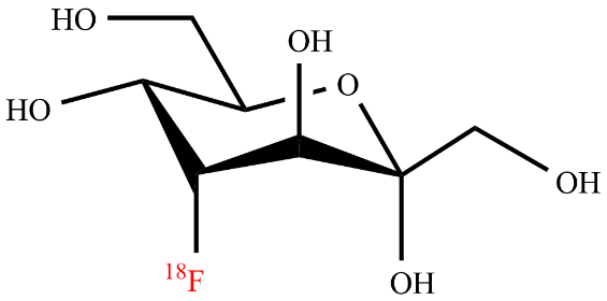

Figure 13: Structure of 4-Deoxy-4-fluoro-D-sedoheptulose in pyranose chair conformation

The third aim of this thesis is to synthesize a protected and fluorinated sedoheptulose derivative as a reference compound to verify product formation after the attempted radiosynthesis of [^{18}F]-

4-deoxy-4-fluorosedoheptulose. Figure 14 shows the structure of the target compound with a fluorine atom at position 4 of the carbohydrate scaffold.

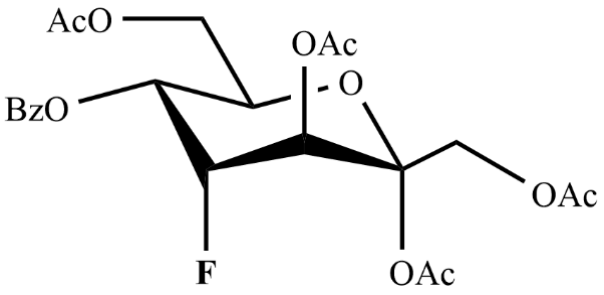

*Figure 14: Structure of planned reference compound 1,2,3,7-tetra-O-acetyl-5-O-benzoyl-4-*fluoro-*D-glycero-α-D-lyxo-hept-2-ulopyranose in pyranose chair conformation*

Results and Discussion

Preliminary “cold” fluorination experiment

In a preliminary experiment, it was attempted to attach fluorine-19 to the precursor. This experiment was used to practice the working steps of the radiolabeling experiments before working with radioactive fluorine-18. The chosen reagents for this preliminary experiment were adapted from typical reagents for classic radiolabeling procedures. Potassium fluoride was chosen as the fluoride source. One equivalent of KF was dissolved in 1.5 mL H_2O. The fluoride ion was then trapped on an anion exchange cartridge (PS-HCO_3^-). It was eluted from the cartridge using 0.7 mL of a solution consisting of: 440 mg Kryptofix 2.2.2, 90 mg K_2CO_3 in 20 mL ACN/H_2O (80/20%). Then azeotropic drying was performed. For this purpose, the solution was evaporated at 110°C and 0.8 mL of acetonitrile was added three times under a stream of nitrogen gas. Subsequently, 5 mg of precursor in 250 µL acetonitrile was added to the dried fluoride. The reaction vessel was sealed tightly, and then heated to 85°C for 30 minutes. Samples of the crude reaction mixture (100 µL) were taken after 10, 20 and 30 minutes. The samples were diluted in a 1:20 ratio with the chosen solvent system for HPLC analysis (ACN/H_2O 80/20%). For analysis two analytical HPLC columns were used (see experimental part for details on columns and detection). Figures 15 and 16 show two representative HPLC chromatograms after 10 minutes reaction time. Obtained retention times are given in Table 2.

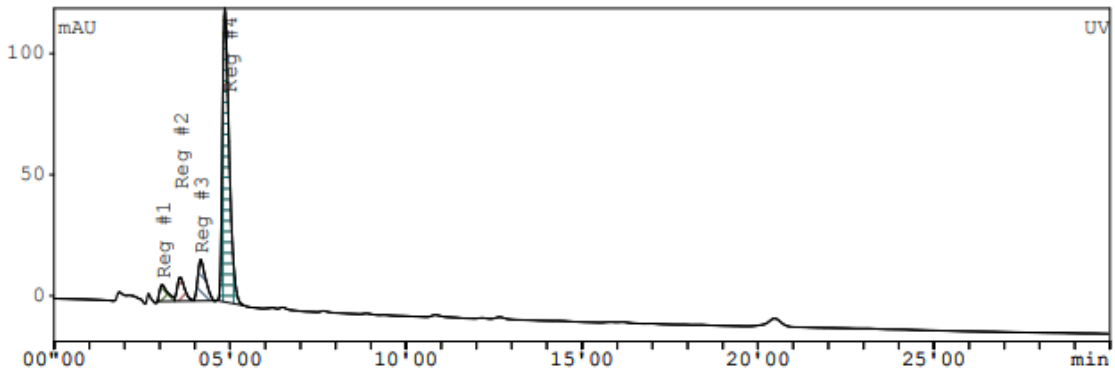

Figure 15: Representative HPLC chromatogram of cold fluorination test synthesis after 10 minutes reaction time (column: Phenomenex RP-C18 Aqua; λ=254 nm solvent: ACN/H_2O = 80/20%; flow: 1 ml/min)

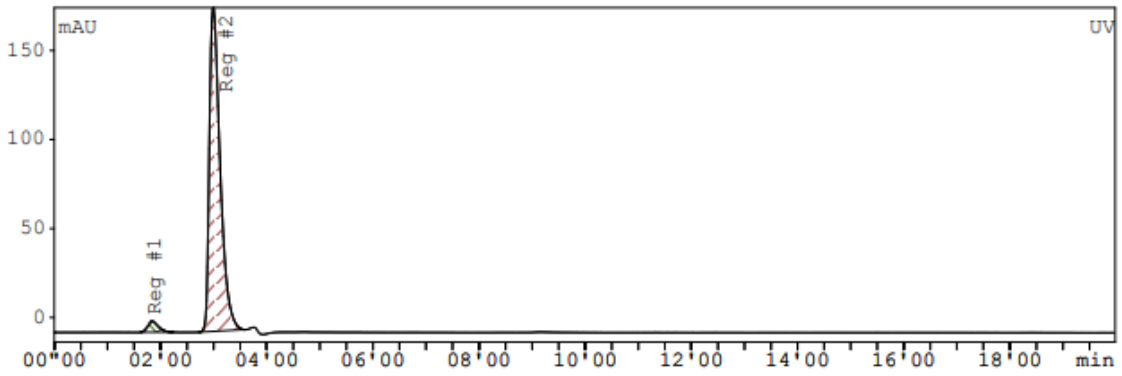

Figure 16: Representative HPLC chromatogram of cold fluorination test synthesis after 10 minutes reaction time (column: Cosmosil Sugar-D; λ=254 nm; solvent: ACN/H2O = 80/20%; flow: 1 ml/min)

Table 2: Obtained Retention times of preliminary "cold" fluorination attempts

Column	**Retention time [min]**
Phenomenex© C-18 Aqua	Reg #1: 2‘58 Reg #2: 3‘34 Reg #3: 4‘10 Reg #4: 4’51
Cosmosil© Sugar-D	Reg #1: 1’51 Reg #2: 3’00

In this preliminary experiment it could not be clearly determined whether the fluorination reaction worked as envisioned. The HPLC chromatogram derived from the precursor showed a peak at 4’53 (see next chapter). The peak Reg #4 (Figure 16) with a retention time of 4’51 in the cold test synthesis indicated that almost no conversion towards the desired product could be achieved. Therefore, the attempt towards a “cold” fluorination was abandoned. In further experiments, which are described in the next chapter, it was attempted to fluorinate the precursor with [^{18}F]fluoride. This may ease the interpretation of the chromatograms and further elucidate the reaction mechanism.

HPLC and TLC analysis of reference compound 4-deoxy-4-fluoro-D-sedoheptulose (4-FDS) and the precursor

Reference Compound 4-FDS

Scheibelberger *et al.* synthesized the respective reference compound of 4-deoxy-4-fluoro-D-sedoheptulose. The reference compound was provided as an aqueous solution (c = 0.1 mol/L). 4-FDS standard was analyzed via HPLC and TLC. The conditions for the development of the radio-TLC plates were adapted from the quality control procedure of [^{18}F]FDG. Figure 17 shows the obtained HPLC chromatogram (Phenomenex Aqua column). Figure 18 shows the HPLC chromatogram of the standard compound with the Cosmosil Sugar-D column. The analytical data of the 4-FDS standard is summarized in Table 3.

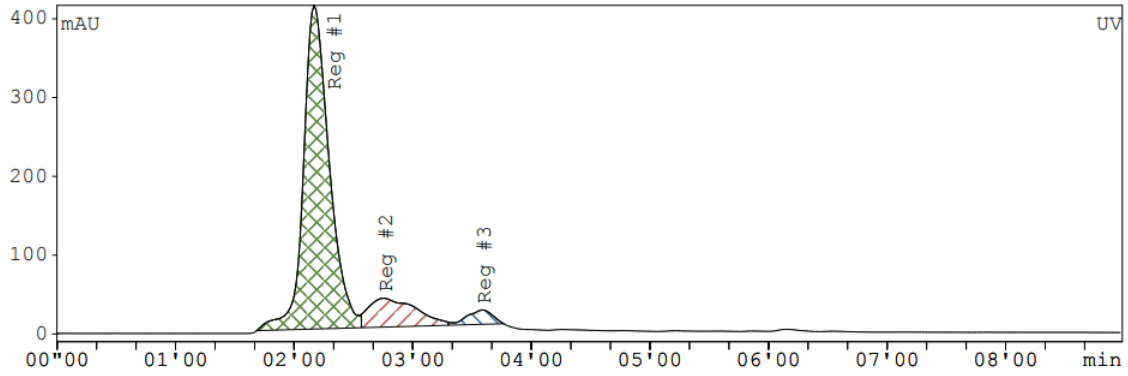

Figure 17: HPLC chromatogram of 4-FDS standard (c = 0.1 mol/L). (column: Phenomenex© RP C18 Aqua; λ=254 nm; solvent: ACN/H₂O = 80/20%; flow: 1 ml/min)

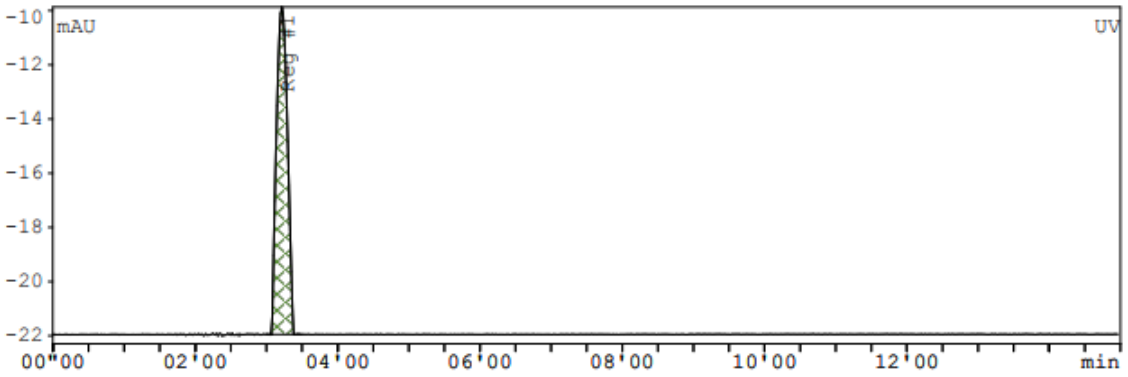

Figure 18: HPLC chromatogram of 4-FDS standard (c = 0.1 mol/L). (column: Cosmosil© Sugar-D; λ=254 nm; solvent: ACN/H₂O = 80/20%; flow: 1ml/min)

Table 3: Analytical data of HPLC chromatograms of 4-FDS standard (solvent: ACN/H_2O = 80/20%; flow: 1ml/min) and TLC chromatogram (solvent: ACN/H_2O = 95/5%; staining reagent: CAM)

Method	**Analytical data**	
HPLC	Column: Phenomenex© RP C18 Aqua Retention time [min]: Reg #1: 2'10 Reg #2: 2'45 Reg #3: 3'35	Column: Cosmosil© Sugar-D Retention time [min]: Reg #1: 3'13
TLC	R_f value: 0.52	

The HPLC chromatogram of the reference compound (Figure 17) with the Phenomenex© Aqua column showed three peaks. The main peak is Reg #1 with a retention time of 2'10. The two minor peaks Reg #2 and Reg #3 could not be clearly identified. The peaks could show impurities in the standard solution or different epimers of the standard compound.

The HPLC chromatogram of the reference compound with the Cosmosil© Sugar-D column (Figure 18), showed one peak with a retention time of 3'13.

Precursor

The precursor was analyzed *via* HPLC and TLC. Figure 19 shows the measured HPLC chromatogram with the Phenomenex Aqua column. Figure 20 shows the HPLC chromatogram with the Cosmosil Sugar-D column. The analytical data of the analysis is summarized in Table 4.

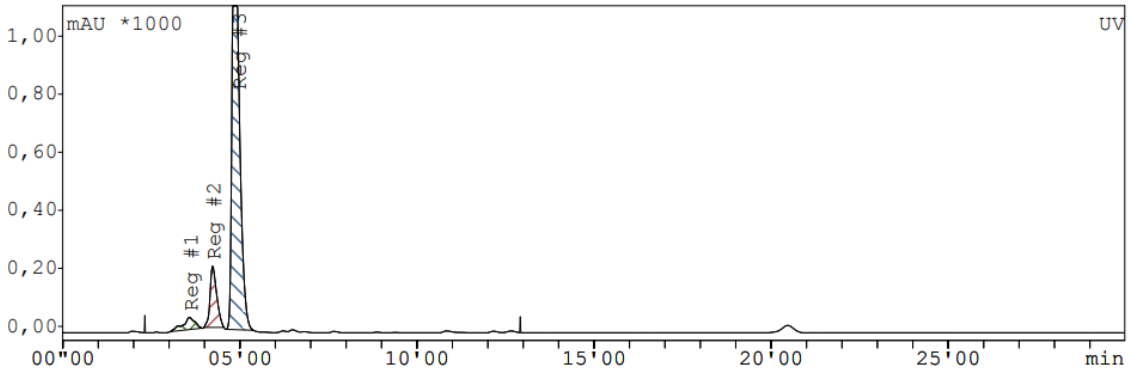

Figure 19: HPLC chromatogram of Precursor (column: Phenomenex© RP C18 Aqua; λ=254 nm; solvent: ACN/H2O = 80/20%)

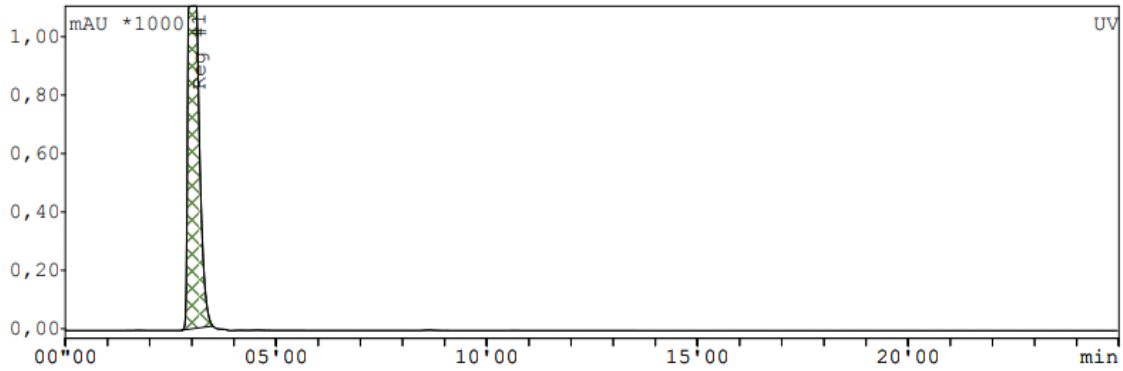

Figure 20: HPLC chromatogram of precursor (column: Cosmosil© Sugar-D; λ=254 nm; solvent: ACN/H2O = 80/20%)

Table 4:Analytical data of the HPLC chromatogram of the precursor (solvent: ACN/H2O = 80/20% and TLC chromatogram (solvent: ACN/H2O = 95/5%; staining reagent: CAM)

Method	**Analytical data**	
HPLC	Column: Phenomenex© RP C18 Aqua Retention time [min]: Reg #1: 3'35 Reg #2: 4'14 Reg #3: 4'53	Column: Cosmosil© Sugar-D Retention time [min]: Reg #1: 3'04
TLC	R_f value: 0.95	

The HPLC chromatogram of the precursor showed three peaks. The main peak was Reg #3 with a retention time of 4'53. The analytical data of the HPLC analysis (Phenomenex Aqua column) indicate that the 4-FDS (retention time: 2'10 min) and the precursor (retention time: 4'53) can be separated with the chosen solvent system. The HPLC chromatograms for the standard and the precursor measured with the Cosmosil Sugar-D column (Figure 20 and 21) show only one peak each. Unfortunately, the retention times of 3'13 (standard) and 3'04 (precursor) were too similar to ensure good separation. Therefore, it was decided to use the Phenomenex© Aqua column for future HPLC analysis.

The TLC chromatograms showed that the solvent system is suitable for separation of the precursor and the final product. Generally, it is beneficial to use both analytical methods to characterize the products of a radiolabeling test synthesis. TLC chromatography is very valuable, since the "naked" fluoride-18 ion cannot be detected *via* HPLC. Therefore, both analytical methods were used to determine whether the radiolabeling and deprotection of the product was successful.

Radiofluorination

The radiolabeling procedures towards 4-[^{18}F]fluoro-deoxy-D-sedoheptulose were performed following the reaction scheme in Figure 21 below:

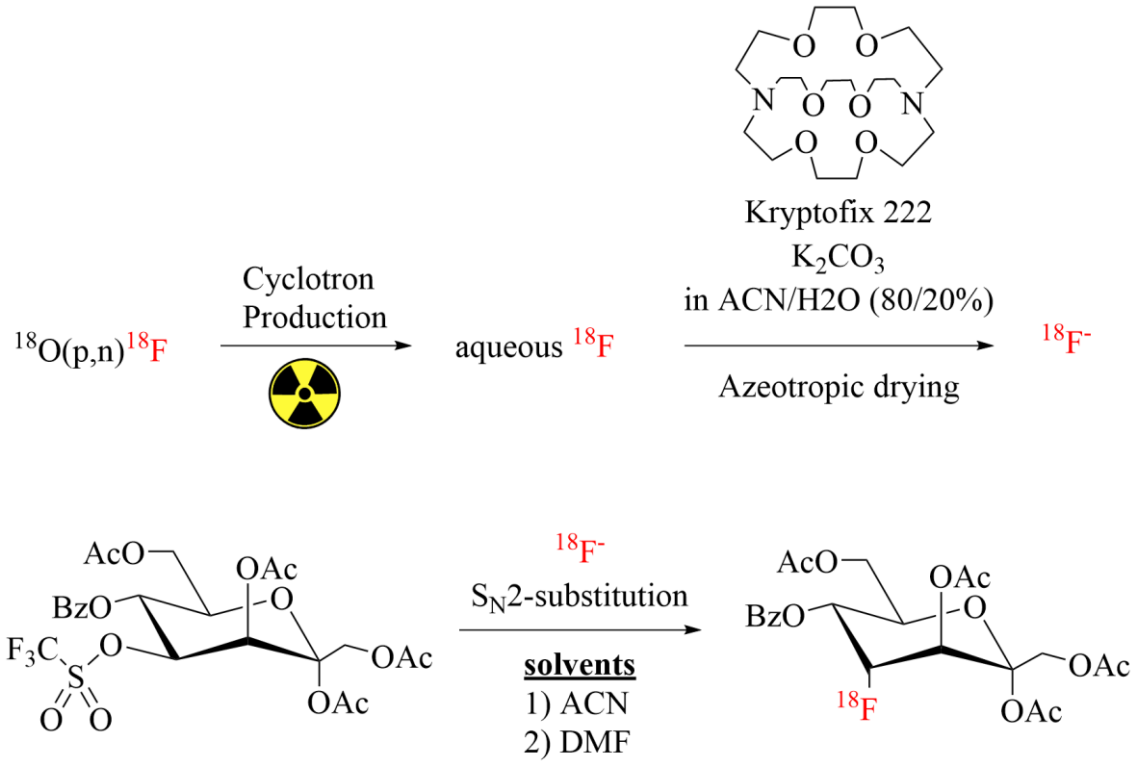

Figure 21: Reaction scheme for 4-[18F]FDS

For the first test synthesis, a small-scale reaction in acetonitrile at 75°C was performed. After cyclotron production of [^{18}F]fluoride, the cyclotron was rinsed with H_2O. 2.0 mL of the aqueous solution containing [^{18}F]fluoride, was transferred into a Wheaton vial. The aqueous solution was then passed through an anion exchange cartridge (PS-HCO_3^-) to trap the [^{18}F]fluoride. The [^{18}F]fluoride was then eluted using 0.7 mL of Kryptofix222/K_2CO_3 solution (for detailed information see the experimental part section "General procedure for radiolabeling and deprotection of 4-FDS"). For the removal of residual water, the [^{18}F]fluoride was azeotropically dried by three time addition of 0.7 mL acetonitrile and heating to 110°C. Then, precursor (c = 38 mg/mL) was added to the dried [^{18}F]fluoride. The reaction vessel was tightly sealed, and the reaction mixture was heated to 75°C. The synthesis was started with an activity of 91.54 MBq. Samples (5 µL) of the crude reaction mixture were taken every 10 minutes, diluted with 95 µL ACN/H_2O = 80/20% solution and then analysed *via* HPLC. Radio TLC chromatograms were performed with 5 µL of the crude reaction mixture.

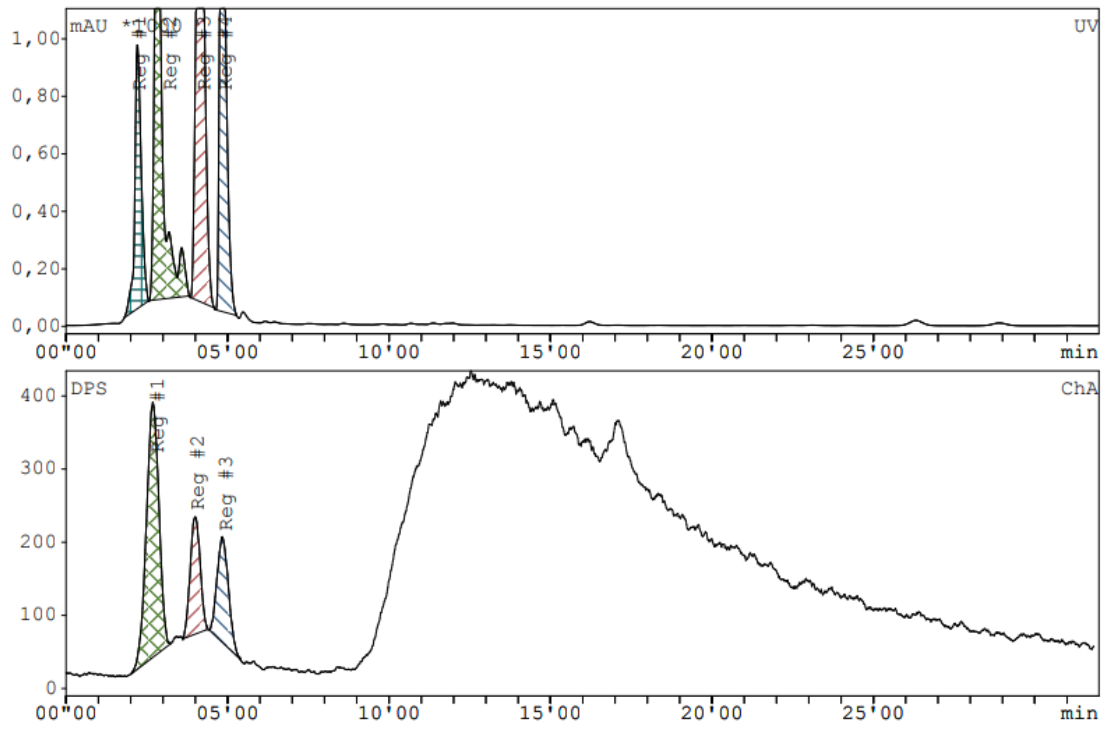

Figure 22: Representative HPLC chromatogram of first radiolabeling test synthesis after 10 minutes reaction time. The top half shows the obtained signals in the UV-channel. The bottom half shows the obtained signals in the radio-channel (column: Phenomenex© RP C18 Aqua; λ=254 nm; solvent: ACN/H2O = 80/20%; flow: 1 ml/min)

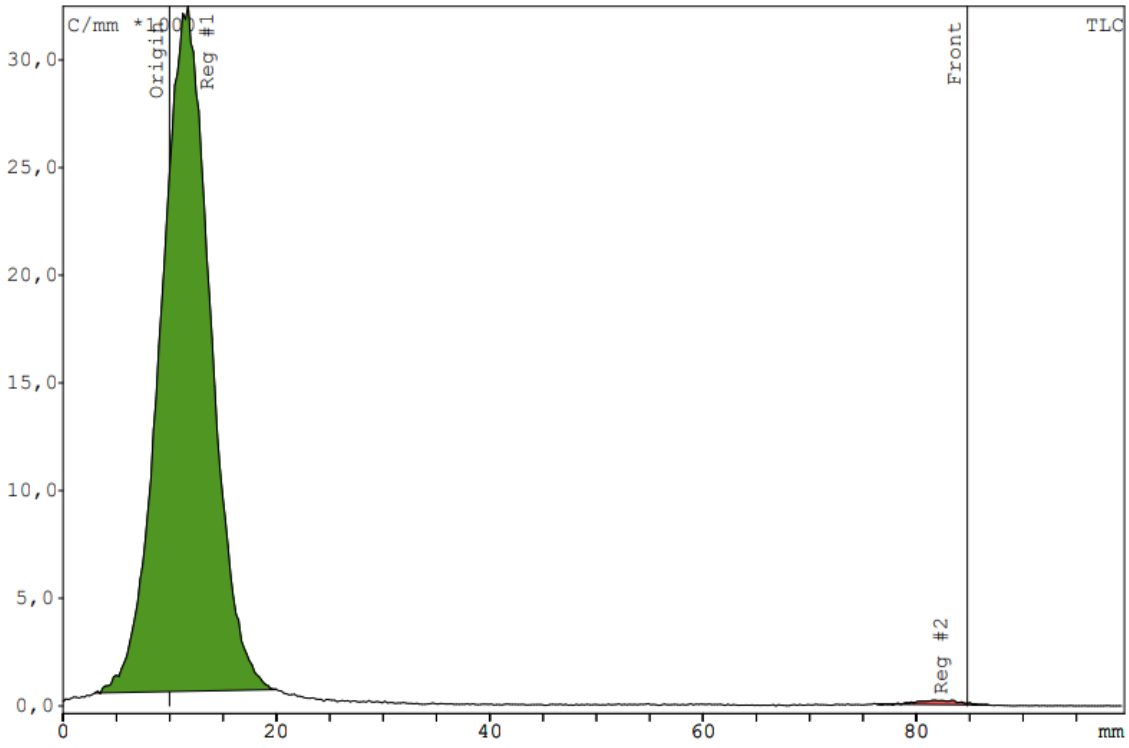

Figure 23: Representative radio-TLC chromatogram of first radiolabeling test synthesis after 10 minutes reaction time. (solvent: ACN/H_2O = 95/5%)

Table 5: Obtained retention times of first radiolabeling test synthesis after 10 minutes reaction time (column: Phenomenex© RP C18 Aqua; λ=254 nm; solvent: ACN/H2O = 80/20%; flow: 1 ml/min)

Column: Phenomenex© RP C18 Aqua	**UV detector**	**RI detector**
Retention time [min]:	Reg #1: 2'13	Reg #1: 2'44
	Reg #2: 2'52	Reg #2: 4'01
	Reg #3: 4'13	Reg #3: 4'45
	Reg #4: 4'53	

Table 5 summarizes the obtained data from the HPLC analysis. The HPLC chromatogram (Figure 22) showed three radioactive signals with retention times of 2'44, 4'01 and 4'54. The peak at 2'52 (UV channel) and 2'44 (RI detector) indicates that a radioactive product was formed, since this peak was not detected in the analysis of the precursor nor the standard solution. The broad peak starting at a retention time of 10'00 (RI channel) is unreacted fluorine-18.

Surprisingly, the retention times of the RI-channel did not correlate with the signals in the UV-channel. Radiochemical conversion was determined via radio-TLC. The green peak in Figure 23 represents unreacted [^{18}F]fluoride (R_f = 0.02). The red peak represents radioactive product (R_f = 0.96). Radio-TLC indicated a very low conversion of only 0.52%. Due to the low conversion, it was decided to heat the reaction mixture to higher temperatures in the following experiments.

Radiofluorination test syntheses in *N,N*-dimethyl formamide

As the boiling point of acetonitrile is 82 °C, DMF (boiling point of 153 °C) was chosen as an alternative solvent for further radiolabeling tests, to avoid evaporation of solvent during the reaction.

The reaction was set up as described for the experiments in acetonitrile. Precursor (4.32 mg in 100 µL DMF) was added to dried [^{18}F]fluoride in a 1.5 mL Wheaton vial. The starting activity of the synthesis was 66.96 MBq. The reaction mixture was heated to 85 °C for 50 minutes. Samples (5 µL) were taken every 10 minutes and analysed with radio-TLC to determine the conversion. Table 6 shows the increasing conversion rates with reaction time.

Table 6: Results of first radiolabeling test synthesis in DMF. Conversion was determined via radio-TLC through comparison with peak of unreacted [^{18}F]fluoride.

Reaction time [min]	**R_f value**	**Conversion [%]**
10	0.81	1.38
20	0.84	1.55
30	0.83	1.90
40	0.80	2.39
50	0.91	5.14

The higher reaction temperature and longer reaction time improved the conversion towards the desired radiolabeled product. To further increase conversion rates, the reaction was then performed at 105 °C.

For the reaction, precursor (48.80 mg/mL) in DMF was added to dried [^{18}F]fluoride. The starting activity was 61.80 MBq and the reaction time 30 minutes. Samples (5µL) were taken every 10 minutes and analysed with radio-TLC. Figure 24 shows a radio-TLC chromatogram after 30 minutes reaction time. Table 7 shows the results from the first radiolabeling attempt at 105 °C reaction temperature.

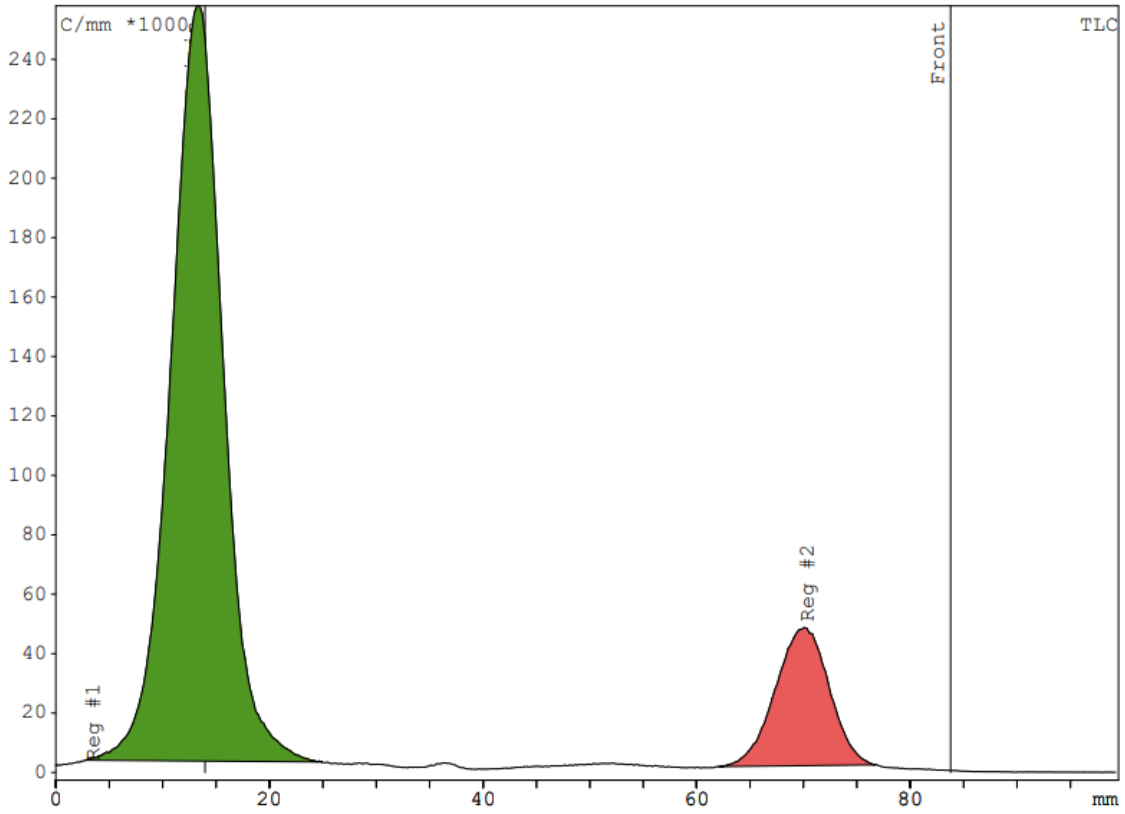

Figure 24: Representative radio-TLC chromatogram of radiofluorination test synthesis at 105 °C after 30 minutes reaction time (solvent: ACN/H_2O = 95/5%)

Table 7: Results of first radiolabeling test synthesis at 105 °C. Conversion was determined via radio-TLC through comparison with peak of unreacted [^{18}F]fluoride.

Reaction time [min]	**R_f value**	**Conversion [%]**
10	0.80	15.78
20	0.82	16.06
30	0.81	21.08

With the chosen reaction conditions a conversion of up to 21 % was achieved. Therefore, it was decided to try to reproduce the results with these reaction conditions.

All results of the radiolabeling experiments are shown in Table 8 below.

Table 8: Results from radiolabeling test syntheses. Conversion was determined via radio-TLC. (Starting activity: Activity before precursor addition).

Precursor concentration [mg/mL]	**Starting activity [MBq]**	**Reaction Temperature [°C]**	**Retention factor**	**Conversion [%]**	**Solvent**
48.02	61.80	105	0.863	21.08	DMF
43.21	66.95	85	0.910	5.14	DMF
57.45	153.60	110	0.985	0.99	DMF
45.73	248.50	110	0.902	9.95	DMF
17.11	649.50	105	0.882	6.58	DMF
21.19	120.90	105	0.901	3.60	DMF
21.05	121.20	105	0.971	0.45	DMF
8.64	72.52	105	0.954	2.82	DMF
41.40	29.34	105	0.969	2.85	DMF

As illustrated in Table 7, the results of the radiolabeling attempts could not be reproduced. Although conversion towards a product was always achieved, the conversion rates did not exceed 10%. This may be caused by the stability of the precursor. NMR analysis of the precursor showed a peak at $\delta = 2.75$ ppm, which corresponds to a hydroxy group at position 4 in the carbohydrate scaffold. This indicates that the triflate leaving group is cleaved off the molecule, when the molecule is repeatedly exposed to moisture. To avoid this problem, it would be beneficial to store the precursor under argon directly after its synthesis and avoid contact with air and moisture.

Although the conversion rates could not be reproduced, efforts towards deprotection of the radiolabeled product were performed. This decision was made, because at this point of the thesis no reference standard of the radiolabeled and protected molecule was available. It was envisioned that deprotection of the molecule would enable verification whether the right product was synthesized in the radiolabeling experiments. The deprotection attempts are shown and discussed in the following chapter.

Test syntheses for deprotection of 1,2,3,7-tetra-O-acetyl-5-O-benzoyl-4-[^{18}F]fluoro-D-glycero-α-D-lyxo-hept-2-ulopyranose

A synthetic procedure towards and efficient, fast and quantitative deprotection of the radiolabeled product was established. Deprotection of the radiofluorinated product was attempted as shown in Figure 25.

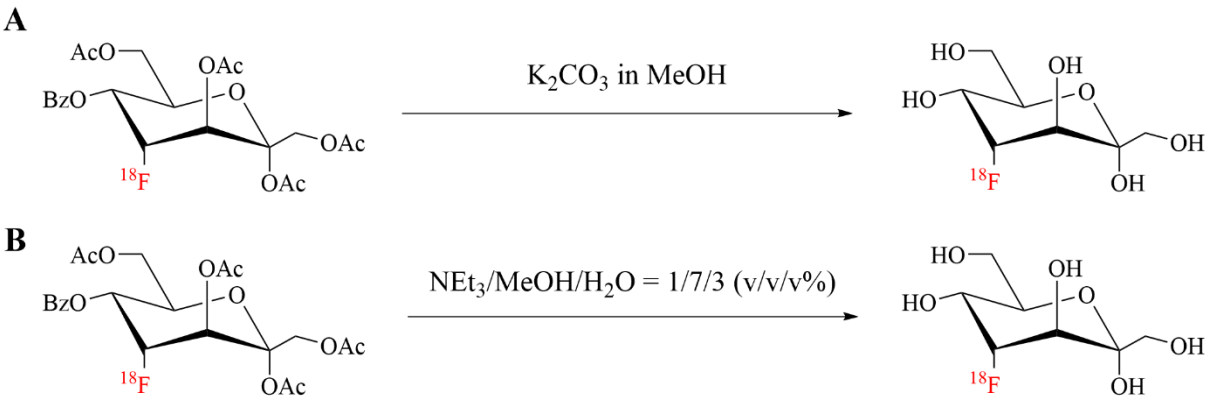

*Figure 25: Scheme of the two approaches towards deprotection of 1,2,3,7-tetra-O-acetyl-5-O-benzoyl-4-[^{18}F]fluoro-D-glycero-α-D-lyxo-hept-2-ulopyranose. **A:** K_2CO_3= potassium carbonate; **B:** MeOH= methanol, NEt_3= triethylamine.*

After radiofluorination at 105°C in DMF, the crude reaction mixture was quenched with 5 mL of H_2O. Through the addition of water, the reactivity of the unreacted [^{18}F]fluoride is significantly decreased. Before deprotection, a separation of the product and [^{18}F]fluoride was performed. The quenched reaction mixture was passed through a preconditioned (see experimental part for conditioning procedure) Sep-Pak© C-18 cartridge. The [^{18}F]fluoride was eluted from the cartridge via three time rinsing with 5 mL water. The product was then eluted into a 2 mL Wheaton vial with 1.5 mL ethanol. Figure 26 shows a radio-TLC chromatogram of the aqueous solution after cartridge separation.

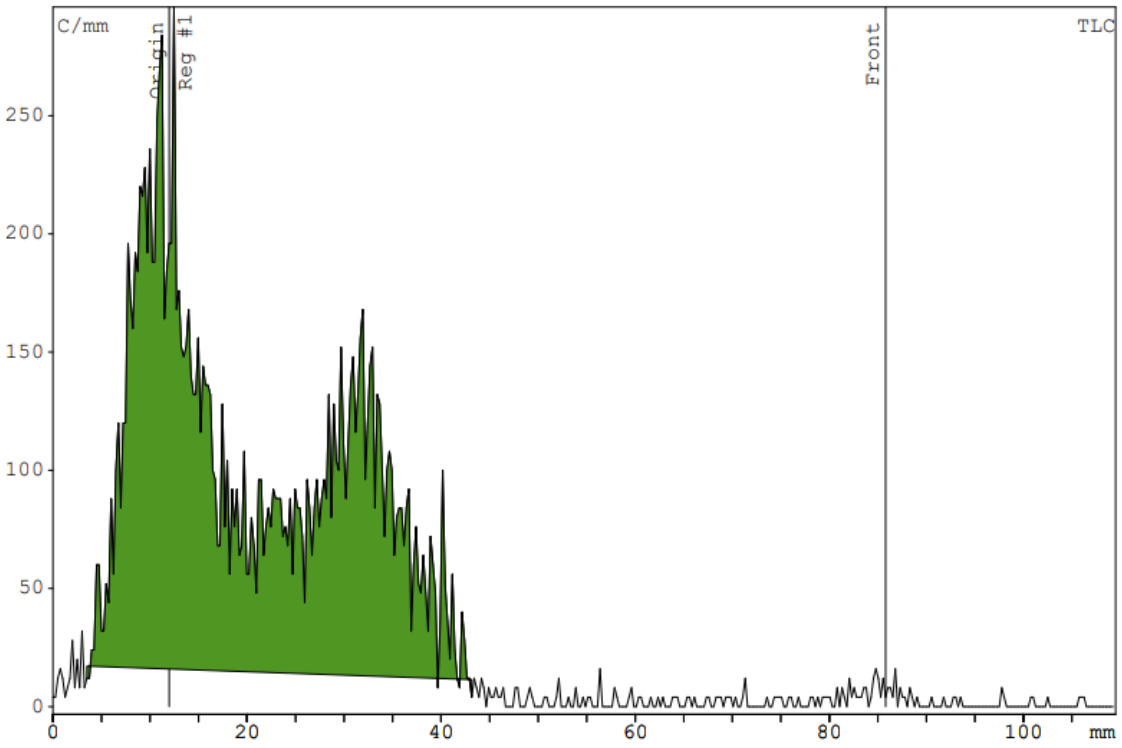

Figure 4: Radio-TLC chromatogram of washing solution after Sep-Pak C-18 separation (solvent: ACNN/H_2O = 95/5%).

As illustrated in Figure 26, no radiolabeled product was found in the aqueous solution. This indicates that the separation of [^{18}F]fluoride and radiolabeled product via the cartridge is feasible. Figure 27 shows a representative radio-TLC of eluted product in ethanol.

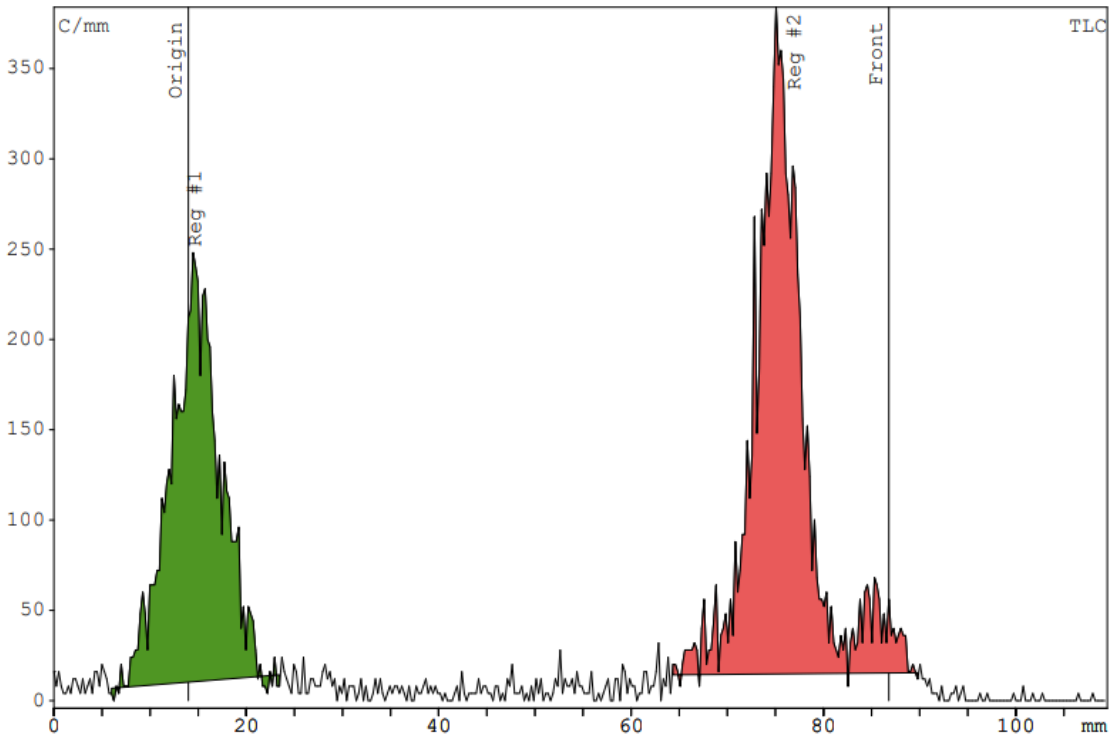

Figure 27: Radio-TLC of the radiolabeled product in ethanol after Sep-Pak C-18 separation (solvent: ACN/H_2O = 95/5%).

Residual amounts of [^{18}F]fluoride were found in the elution solution. Increasing the amount of washing steps could not prevent this issue. This issue may be circumvented by adding additional cartridges or use of a different solution for the elution of the product.

For the first attempts towards deprotection the residual amounts of [^{18}F]fluoride were not considered an issue, because both deprotection solutions contained water.

In preliminary experiments, Scheibelberger *et al.* have shown that the precursor is not stable under acidic and strongly basic conditions (pH < 12).[46] Therefore, the typical conditions for cleavage of acetyl-protecting groups (e.g. 0.1 M HCl or 0.1 M NaOH) were not suitable for the deprotection of the tracer molecule.

The solutions presented in Table 9 have been used for the deprotection experiments of 1,2,3,7-tetra-*O*-acetyl-5-*O*-benzoyl-4-[^{18}F]fluoro-D-glycero-α-D-lyxo-hept-2-ulopyranose to circumvent this issue:

Table 9: Solutions for deprotecting attempts of 1,2,3,7-tetra-O-acetyl-5-O-benzoyl-4-[^{18}F]fluoro-D-glycero-α-D-lyxo-hept-2-ulopyranose

Name	**Solution**	**pH**
E1	Et_3N/Methanol/H_2O (1/7/3 = v/v/v%)	10.1
E2	Saturated K_2CO_3	11.5

In a first test synthesis, the radiolabeled product was eluted from the Sep-Pak© C-18 cartridge with ethanol. The solution was separated into two 750 µL aliquots and the ethanol was evaporated. The residues were dissolved in 50 µL of the respective deprotection solution. The vials were left at room temperature for 10 minutes. Samples were taken after 10 minutes reaction time and analysed via radio-TLC.

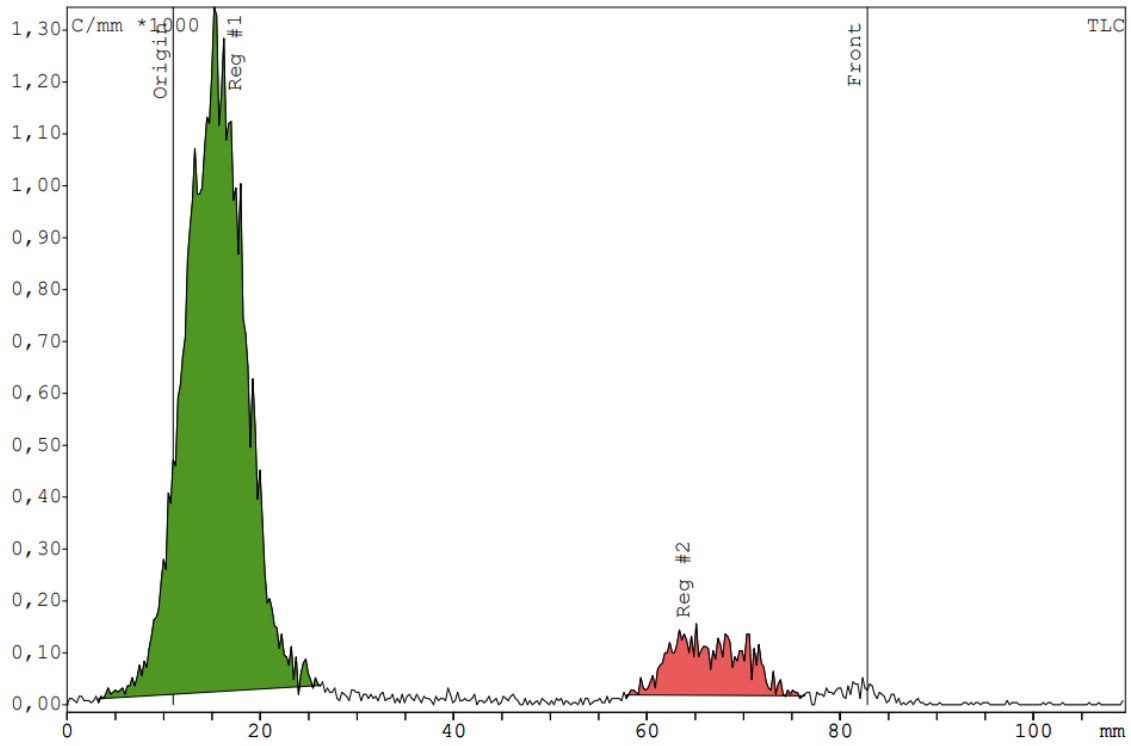

Figure 28: 1,2,3,7-tetra-O-acetyl-5-O-benzoyl-4-[^{18}F]fluoro-D-glycero-α-D-lyxo-hept-2-ulopyranose after deprotection experiment (10 minutes) with E1 solution. (solvent: ACN/H_2O = 95/5%)

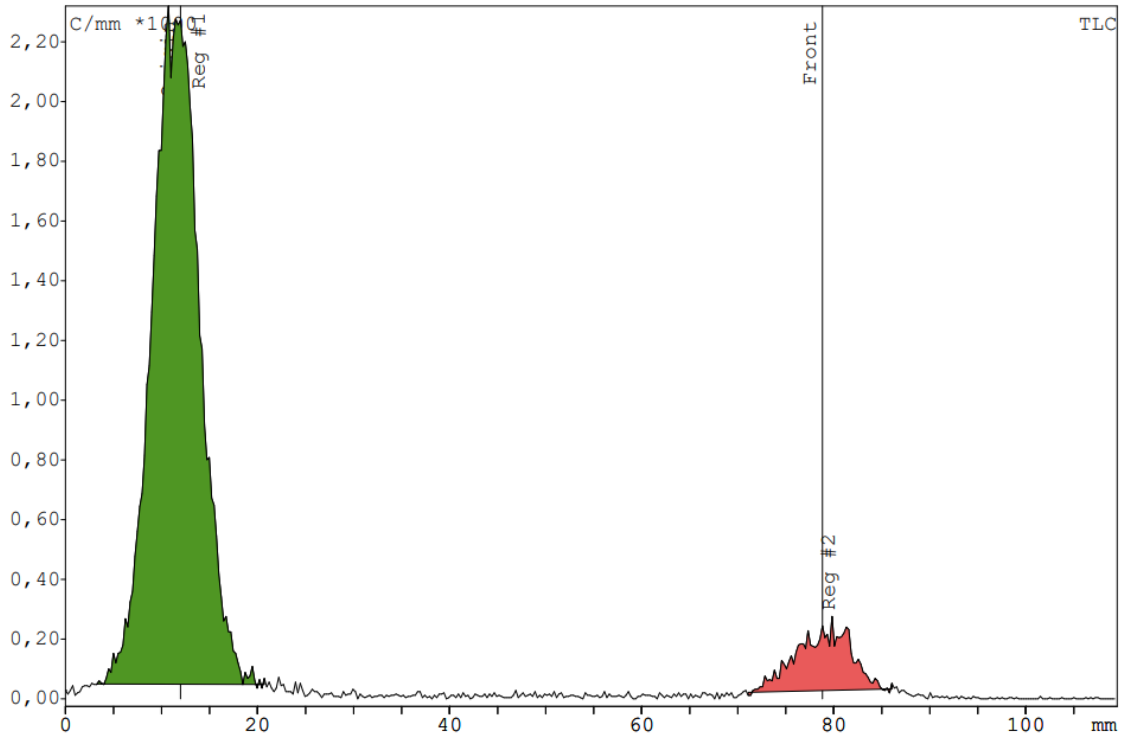

Figure 29: 1,2,3,7-tetra-O-acetyl-5-O-benzoyl-4-[^{18}F]fluoro-D-glycero-α-D-lyxo-hept-2-ulopyranose after deprotection experiment (10 minutes) with E2 solution. (solvent: ACN/H_2O = 95/5%)

The two representative Figures (28 and 29) show the obtained radio-TLC chromatograms of the first attempts towards deprotection. After treatment with solution E2, the R_f-value of the compound was unchanged compared to the radiolabeled product. This indicates that no

cleavage of the protecting groups occurred. Therefore, the solution E2 was not used in further deprotecting attempts.

After treatment with solution E1, the obtained radio-TLC shows a shift towards the R_f-value of the standard compound 4-FDS ($R_f = 0.52$). This indicates that solution E1 is suitable for the deprotection of the radiolabeled product. Unfortunately, the R_f-value did not match the one of the standard compound, which suggests that not all protecting groups were cleaved with the chosen reaction conditions. Due, to the lability of the two different protection groups (acetyl- and benzoyloxy-) it is suggested that only the acetyl-groups could be cleaved with solution E1, and the benzoate-group remains in the molecule. Heating of the reaction mixture up to 85°C during deprotection, also did not lead to full deprotection of the radiolabeled product.

Synthetic strategy towards 1,2,3,7-tetra-*O*-acetyl-5-*O*-benzoyl-4-fluoro-D-glycero-α-D-lyxo-hept-2-ulopyranose as a reference compound

The characterisation of the radiofluorinated sedoheptulose intermediate posed difficulties, since only the precursor molecule and a standard solution of the final product were available. Thus, there was no analytical data for the radiolabeled intermediate to compare the results from the radiolabeling experiments with. Therefore, a synthetic strategy towards a reference compound of the radiolabeled intermediate was established. The envisioned strategy is shown in Figure 30 and will be discussed in the following chapter.

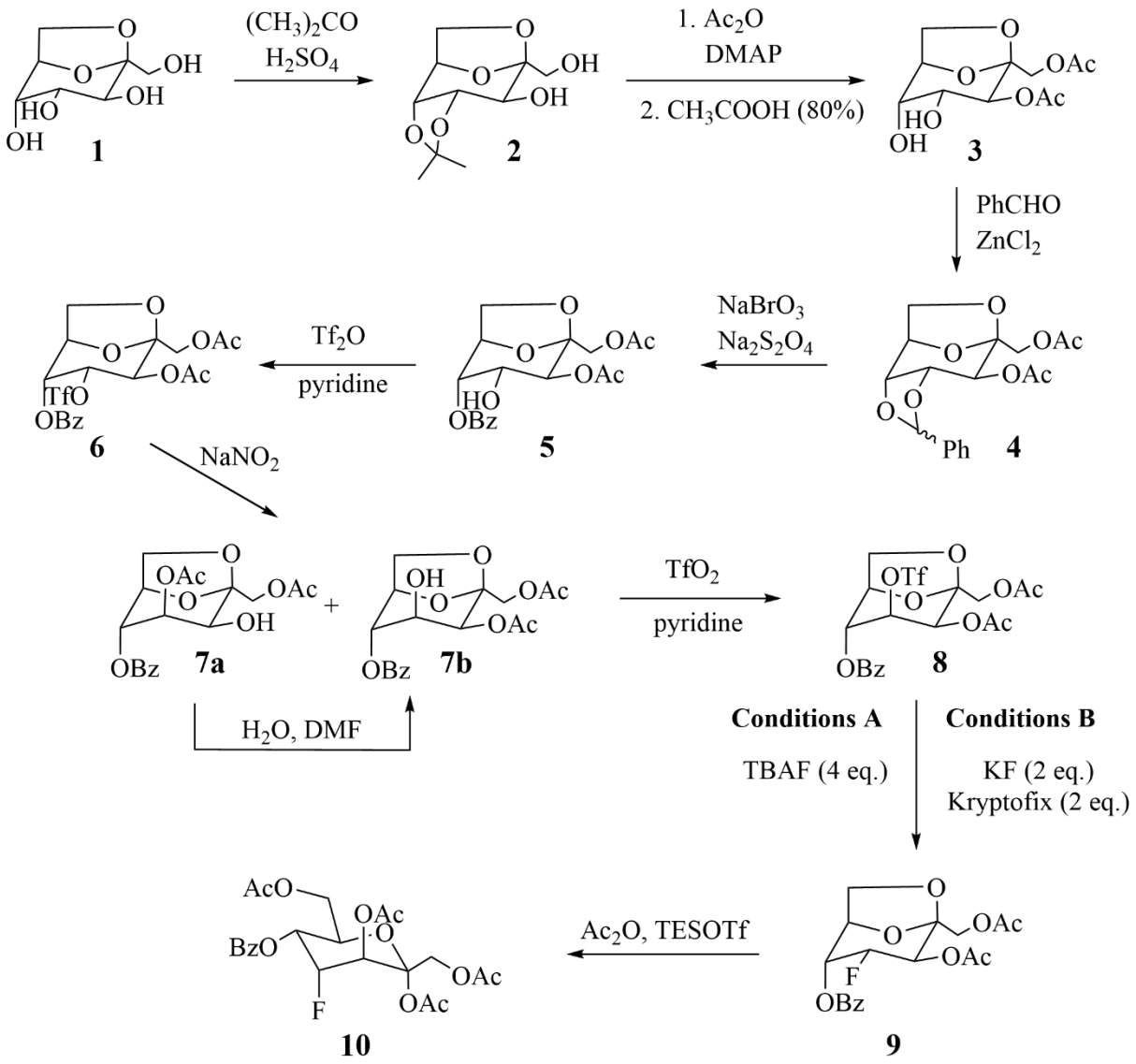

Figure 30: Envisioned synthetic strategy of a fluorinated reference compound bearing protecting groups starting from commercially available sedoheptulose anhydride.

The synthesis started from commercially available sedoheptolusan monohydrate (2,7-anhydro-D-sedoheptulose; Compound **1**). The reactions were done on a 500 mg scale of sedoheptolusan monohydrate. First, sedoheptulosan monohydrate was selectively isopropylidene protected at position 4 and 5 by dissolving sedoheptulosan monohydrate in dry acetone and stirring it at room temperature for 3 h under acidic conditions (Compound **2**). Then an acetylation of the vicinal hydroxy groups at position 1 and 3 was performed using acetic anhydride and a catalytic amount of *N,N*-(dimethylamino)pyridine (DMAP) to protect these positions from further reactions. Subsequently, the isopropylidene protecting group was removed with aqueous acetic acid at 80°C (Compound **3**). The two hydroxyl groups at position 4 and 5 were then protected again with a benzylidene acetal using benzaldehyde under Lewis-acid catalysis with zinc chloride (Compound **4**). Scheibelberger at al. showed that purification on silica gel led to partial decomposition of the benzylidene protected product, therefore remaining benzaldehyde was removed at 80°C on a rotary evaporator for 4h. The benzylidene acetal was incorporated, since benzoate protecting groups are known to prevent acetyl-migration, which proofed to be beneficial in the following Lattrell-Dax epimerization (see reaction of compound **6** to compound **7a** and **7b**).

Over the first 4 steps of the reaction scheme 615.7 mg of pure 1,3-di-*O*-acetyl-2,7-anhydro-4,5-*O*-benzylidene-D-glycero-β-D-arabino-hept-2-ulopyranose could be obtained from 500 mg of sedoheptulosan monohydrate which corresponds to an excellent yield of 71%. Additionally, only one recrystallisation step needed to be done during the first 4 steps and no chromatographic purification was necessary.

The benzylidene acetal was opened under oxidative conditions using sodium dithionite and sodium bromate in a biphasic mixture of water and ethyl acetate to yield the key synthetic intermediate 1,3-di-*O*-acetyl-2,7-anhydro-5-*O*-benzoyl-D-glycero-β-D-arabino-hept-2-ulopyranose (Compound **5**).[47]

Unfortunately, the stereocenter at the now unprotected position 4 of the carbohydrate needed to be inverted to ensure overall retention of the configuration after fluorination. Scheibelberger *et al*. examined several procedures for the inversion of the stereocenter at position 4 of the carbohydrate scaffold.

They reported the best results for the inversion of the stereocenter by a Latrell-Dax-epimerization. The Latrell-Dax epimerization is a nitrite-mediated substitution of carbohydrate triflates and poses an efficient method to generate structures with inverse configuration under mild conditions.[28]

For the Latrell-Dax epimerization the synthetic intermediate 1,3-di-*O*-acetyl-2,7-anhydro-5-*O*-benzoyl-D-glycero-β-D-arabino-hept-2-ulopyranose (Compound **5**) was treated with trifluoromethanesulfonic anhydride and pyridine in dry *N*,*N*-dimethylformamide for 1h at 0°C to give triflate (Compound **6**) in an excellent yield of 94%. The subsequent reaction of the carbohydrate triflate (**6**) with sodium nitrite under an argon atmosphere for 72h led to a 1:1 mixture of desired product (**7b**) and undesired migration product (**7a**).

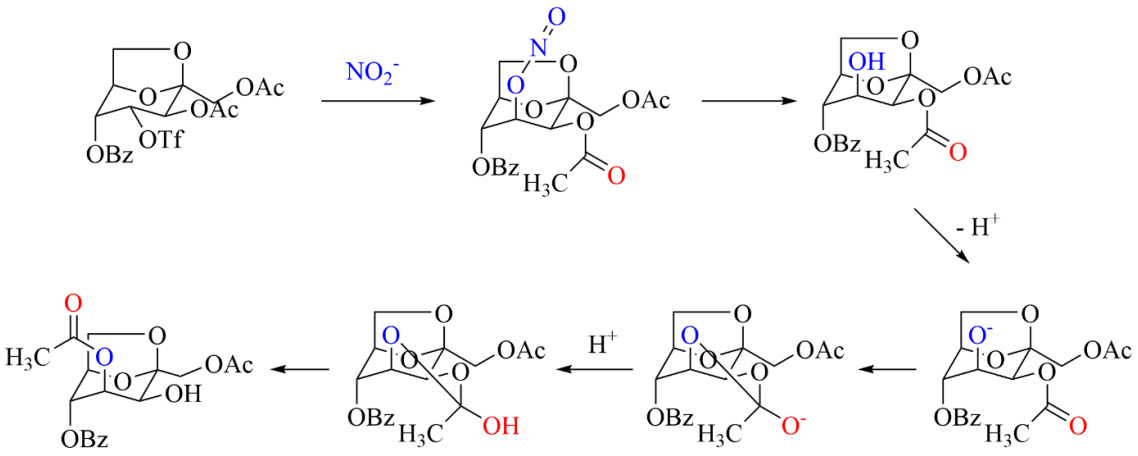

Figure 31: Proposed mechanism of acetyl-group migration during Lattrell-Dax epimerization

Figure 31 shows a proposed mechanism for the acetyl-migration, during the Lattrell-Dax epimerization. First, the nitrite ion attacks carbon 4 and substitutes the triflate group. Subsequently, an acyloxonium ion is formed and the acetyl-group migrates from carbon 4 to carbon 3, yielding the undesired migration product **7a**. Surprisingly, by monitoring the reaction via NMR spectroscopy Scheibelberger *et al*. revealed that the undesired epimer is formed first and the acetyl group migrates back from position 4 to position 3 over the course of the reaction until the equilibrium is reached. The following separation of the two epimers proofed to be difficult. First it was tried to separate the epimers via manual column chromatography with the solvent system *n*-heptane/ethylacetate in a ratio of 1:1. Unfortunately, only unreacted triflate (**6**) could be separated from the two epimers, because the difference of 0.05 in the R_f-values of the products was too small to separate these two compounds by isocratic elution. Additionally, it was attempted to separate the epimers via a preparative thin-layer chromatography using the same solvent system, but this approach also did not lead to sufficient purification.

Since it was not possible to separate the epimers through isocratic elution, a gradient elution via an MPLC system was done. The gradient elution using 12%-46% ethylacetate in toluene established by Scheibelberger et al. was attempted, but no efficient separation could be achieved using this solvent system. Finally, separation was achieved using a gradient of 15%-60% ethylacetate in toluene, yielding the desired pure epimer (**7b**) with moderate yields of 24%.

Pure compound **7a** was then stirred in wet DMF for 72h, to again reach an equilibrium of 1:1 with desired compound **7b**. Following this procedure the yield of desired product **7a** could be improved.

After successful epimerization the product with the desired stereochemistry **7a** was treated with trifluoromethanesulfonic anhydride and pyridine to give the carbohydrate triflate in an excellent yield of 86%.

Compound **8** was used as a starting material to synthesize the desired fluorinated carbohydrate. First, it was attempted to mimic the reaction conditions of a classic radiofluorination reaction. For this purpose, potassium fluoride was used as a fluoride source and Kryptofix 2.2.2 was used as a cryptand. Both reagents were added in excess (2 equiv.) to enable faster reaction times and push the equilibrium of the proposed substitution reaction towards the desired product. The chosen temperatures for the reaction ranged from 50°C to 110°C.

The ^{19}F-NMR spectra showed a signal at -77 ppm, which corresponds to the fluoride atoms in a triflate-group. The expected shift of a fluoride atom connected to a secondary carbon (-180 ppm to -210 ppm) could not be detected (Figure 32). The calculated mass for the desired compound **9** was neither detected by mass spectrometry. Therefore, it was concluded that the fluorination was unsuccessful.

Following these results, it was attempted to fluorinate compound **8** with a different fluoride source. Tetrabutylammonium trihydrate showed promising results in the nucleophilic fluorination using mesylates and halides as leaving groups.[48] For this reaction 4 equivalents of tetrabutylammonium trihydrate were used and the reaction temperatures ranged between 70°C and 110°C. The ^{19}F-NMR spectra again showed a shift of -77 ppm, and the calculated mass could not be found.

Figure 32 shows a representative ^{19}F-NMR spectrum in $CDCl_3$, where a single peak at -77 ppm, corresponding to fluorine atoms in a triflate-group can be observed. The spectra were identical for both fluorination strategies.

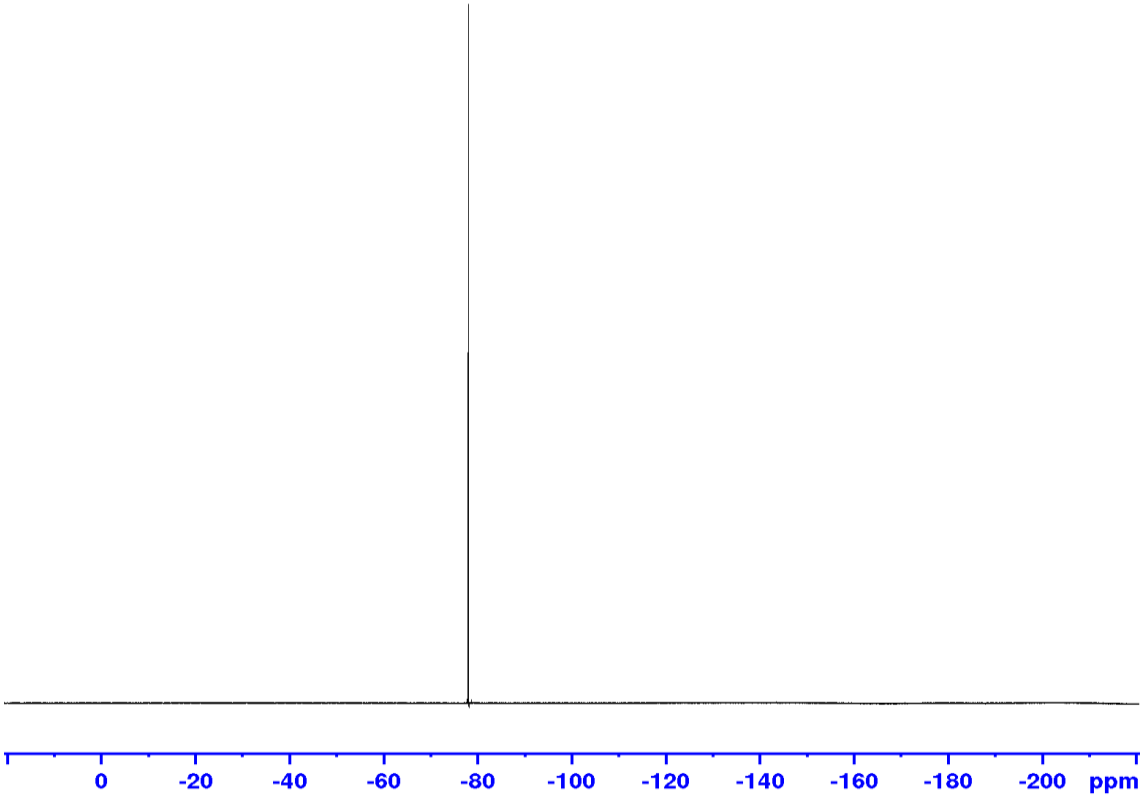

Figure 32: Representative ^{19}F-NMR spectrum in $CDCl_3$ (659 MHz) of compounds 9.1 and 9.2. The peak at -77 ppm corresponds to the fluorine atoms of the triflate group.

Ultimately, it can be said that the chosen approaches for fluorination were not successful under the tested reaction conditions. This may be caused by poor reactivity of the sedoheptulose derivative (compound 8), or the tested reaction temperatures were too low. The ^{1}H-NMR spectra taken after the fluorination attempts indicate that compound **8** is still intact. In future experiments it would be possible to heat the reaction mixture to higher temperatures, in order to achieve conversion. Additionally, other fluoride sources or different cryptands could be tested to enable a successful reaction.

Summary and Outlook

Several small-scale test syntheses regarding the radiofluorination of the precursor 1,2,3,7-tetra-*O*-acetyl-5-*O*-benzoyl-4-*O*-trifluoromethanesulfonyl-D-glycero-α-D-lyxo-hept-2-ulopyranose were performed. The radio-TLC analysis indicated that radiolabeled sedoheptulose was obtained with conversion rates up to 20%. The results were not reproducible, which suggests an optimization of the procedure. First, the stability of the precursor needs to be further examined. Secondly, small-scale reactions in a fully automated synthesis module could be established to achieve reproducibility of the radiolabeling results.

The deprotection attempt with saturated potassium carbonate solution did not work and was abandoned. Deprotection with Et_3N/Methanol/H_2O (1/7/3 = v/v/v%) solution worked only partially, as the obtained R_f values did not match the obtained R_f value of the 4-deoxy-4-fluoro-D-sedoheptulose standard. This indicated that no full deprotection of the molecule could be achieved. It is suggested that the acetyl protecting groups could be cleaved, but the benzoyloxy protecting group remained in the molecule. Elevated temperatures during deprotection did not lead to full deprotection. In future experiments, it is be crucial to achieve full deprotection of the radiolabeled product. This may be achieved via addition of a catalyst or a different deprotection solution.

A nine-step synthesis towards a reference compound for a fluorinated sedoheptulose derivate bearing protecting groups was established. Key steps in the synthetic route were the Latrell-Dax epimerization and the introduction of fluoride as the penultimate step before opening the anhydro bridge. The first seven steps of the synthetic scheme worked, but the introduction of the fluorine could not be achieved. This probably was caused by the reactivity of the sedoheptulose derivative or the chosen fluoride sources. In future experiments, more attention needs to be paid towards the fluorination step. Other fluoride sources need to be examined or the fluoride needs to be inserted at a different step of the synthetic scheme.

Experimental part

Materials and Methods

Materials:

All chemicals were purchased from commercial vendors and were used without further purification.

Methods:

Thin layer chromatography (TLC)

Thin layer chromatography was carried out on Merck© silica gel 60 F_{254} glass plates.

Compound spots were visualized by UV light (254 nm) and by treatment with the staining reagent Cerium ammonium molybdate [CAM]: 2 g $Ce(SO_4)\cdot 4\ H_2O$ and 46 g $(NH_4)_6Mo_7O_{24}\cdot 4\ H_2O$ in 1 L 10% (w/w) aqueous H_2SO_4. The plates were dipped in staining reagent followed by heating with a heat gun.

For the development of the TLC plates the following mobile phases were used:

- 100% ethlyacetate (EA)
- *n*-heptane/EA = 50/50 v/v%
- *n*-heptane/EA = 66/33 v/v%

Medium pressure liquid chromatography (MPLC)

Purification of the compounds was either done manually or with a Biotage© Isolera Prime (*Uppsala, Sweden*) flash purification system using Macherey-Nagel© silica gel 60 (0.04-0.063 mm) in self-packed cartridges.

NMR spectra

^{1}H and ^{19}F NMR spectra were recorded on either a Bruker© AV III HD 700 (^{1}H: 700.38 MHz, ^{19}F: 659.01 MHz) or a Bruker© AV III HD 600 (^{1}H: 600.23 MHz, ^{19}F: 564.79 MHz) spectrometer.

Chemical shifts (δ) are reported in parts per million (ppm) and were referenced to the corresponding residual solvent signals in Proton NMR spectra or an external standard:

^{1}H NMR spectra: $CDCl_3$: $CHCl_3$ (δ_H = 7.26 ppm), *d*$_6$-DMSO: [$(CD_2H)SO(CD_3)$] (δ_H = 2.50 ppm).

^{19}F NMR: external standard $CFCl_3$ (δ_F = 0 ppm)

Coupling constants (*J*) are given in Hz. Signal multiplicity is indicated by one of the following: s (singulet), d (doublet), t (triplet), q (quartet), m (multiplet).

High resolution mass spectra

High resolution mass spectra (HRMS) were recorded on a Bruker maXis UHR-TOF (ultrahigh resolution – time of flight) spectrometer. The samples were ionized with ESI (electrospray ionisation) in positive ion mode.

Production of [^{18}F]Fluoride

[^{18}F]Fluoride was produced in a GE PETtrace cyclotron (GE Medical Systems, *Uppsala, Sweden*) via $^{18}O(p,n)^{18}F$ reaction. For the small-scale test synthesis described in this thesis, no irradiation was performed, but the target was rinsed with H_2O after the routine production of [^{18}F]FDG.

(Radio) high performance liquid chromatography (radio-HPLC)

HPLC analysis was performed via analytical reverse-phased HPLC equipped with a UV- and a radioactivity detector. UV detection was performed at a wavelength of 254 nm. Two columns were used for analysis. A COSMOSIL© Sugar-D column (4.6 ID x 250 mm) and a Phenomenex© Aqua C-18 column (5 µm; 4.6 ID x 250 mm). As a mobile phase HPLC grade acetonitrile and water in a ratio of 80:20 v/v% was used (flow rate of 1 mL/min). Raytest software was used for analysis of the chromatograms.

Samples were prepared as follows: 5 µL of the crude reaction mixture were diluted with 95 µL of the mobile phase. 20 µL of this mixture was injected into the HPLC system.

Radio-thin layer chromatography (radio-TLC)

Radio thin layer chromatography was performed with an Elysia© raytest miniGITA Dual device. For analysis of the chromatograms Gina X software by Elysia© was used. As a stationary phase Merck© silica gel 60 F_{254} aluminium plates were used. As a mobile phase HPLC grade acetonitrile and water were used in a ratio of 95:5 v/v%.

Crude reaction mixture (5 µL) was spotted onto the TLC plate and the plate was developed in a TLC chamber. The dried plates were directly analysed with the radio TLC device.

General procedure for radiolabeling and deprotection of 4-FDS

Small scale reactions were done manually in a lead-shielded fume hood with low levels of initial radioactivity (<1 GBq) to evaluate the reaction conditions.

[^{18}F]fluoride was produced within the cyclotron *via* the reaction ^{18}O(p,n)^{18}F. The cyclotron was flushed with H_2O, and the aqueous solution was eluted into a 2.5 mL Wheaton vial. The [^{18}F]fluoride was trapped on a an anion exchange cartridge (PS-HCO_3^-). The [^{18}F]fluoride was eluted from the cartridge using 0.8 mL of a solution containing Kryptofix 222 (20 mg/ml, mol/mL) and K_2CO_3 (4.5 mg/mL, mol/mL) in ACN/water 80/20% v/v. The elution solution was evaporated completely (110°C), and the residue was azeotropically dried via addition of 0.8 mL ACN for three times under a stream of nitrogen gas.

The precursor was dissolved in either ACN or DMF ($c_{precursor}$ = 17.10–57.00 mg/mL) and the resulting solution was added to the dried [^{18}F]fluoride. The reaction mixture was heated to 105 °C for 10 minutes. During the reaction time, a Sep-Pak C-18 cartridge was conditioned with 10 mL ethanol and 20 mL water. After cooling to room temperature, a small sample (5 µL) of the crude reaction mixture was analysed with radio-TLC.

The crude reaction mixture was then diluted with 5 mL “aqua ad injectabilia” and the resulting mixture was passed through the prepared Sep-Pak C-18 cartridge. The cartridge was rinsed three times with 5 mL portions of water and the product was then eluted into a 2.5 mL Wheaton vial with 1.5 mL ethanol. Ethanol was removed under a stream of nitrogen gas. The residue was dissolved in 50 µL of either NEt_3/MeOH/H_2O = 1/7/3 (v/v/v%) or saturated K_2CO_3 solution. Then, the resulting mixture was stirred for 10 minutes at room temperature. The final product was analysed via radio-TLC (ACN/H_2O = 95/5%).

Synthetic strategy towards a reference compound for radiofluorinated sedoheptulose bearing protecting groups

2,7-Anhydro-4,5-*O*-isopropylidene-D-glycero-β-D-arabino-hept-2-ulopyranose (**Compound 2**)

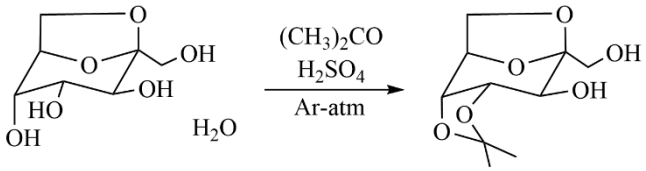

$C_7H_{14}O_7$
210.19 g/mol

$C_{10}H_{16}O_6$
232.23 g/mol

Sedoheptolusan monohydrate (500 mg, 2.38 mmol, 1 equiv.) and molecular sieves (110 mg, 3 Angström) were suspended in dry acetone (4.75 mL) under an argon atmosphere. Then concentrated H_2SO_4 (86.3 mg, 47 µL, 0.88 mmol, 0.37 equiv.) was added and the mixture was stirred at room temperature for 3 h. Over the course of the reaction the colourless suspension turned into a cloudy, white suspension. After the reaction the suspension was filtered and washed three times with cold acetone yielding 2,7-anhydro-4,5-*O*-isopropylidene-D-glycero-β-D-arabino-hept-2-ulopyranose as a greyish solid, which was used for the next step without any purification (514.3 mg, 93%); R_f = 0.29 (EA, CAM); ^{1}H NMR (700 MHz, *d*$_6$-DMSO) δ = 5.14 (d, $^3J_{OH,3}$ = 6.85 Hz, 1H, OH-3), 4.73 (dd, $^3J_{OH,1a}$ = 7.06 Hz, $^3J_{OH,1b}$ = 5.79 Hz, 1H, OH-1), 4.72 (d, $^3J_{6,7b}$ = 5.70 Hz, 1H, H-6), 4.20 (dd, $^3J_{5,4}$ = 6.23 Hz, $^3J_{5,6}$ = 1.29 Hz, 1H, H-5), 4.00 (t, $^3J_{4,5}$ = 6.13 Hz, $^3J_{4,3}$ = 5.91 Hz, 1H, H-4), 3.77 (d, $^2J_{7a,7b}$ = 7.56 Hz, 1H, H-7a), 3.68 (dd, $^2J_{7b,7a}$ = 7.48 Hz, $^3J_{7b,6}$ = 5.42 Hz, 1H, H-7b), 3.60 (dd, $^2J_{1a,1b}$ = 11.90 Hz, $^3J_{1a,OH}$ = 7.06 Hz, 1H, H-1a), 3.54 (dd, $^3J_{3,OH}$ = 6.77 Hz, $^3J_{3,4}$ = 5.65 Hz, 1H, H-3), 3.33 (dd, $^2J_{1b,1a}$ = 11.85 Hz, $^3J_{1b,OH}$ = 5.78 Hz, 1H, H-1b), 1.40 (s, 3H, $CH_3^{isopropylidene}$), 1.28 (s, 3H, $CH_3^{isopropylidene}$).

1,3-Di-*O*-acetyl-2,7-anhydro-4,5-*O*-isopropylidene-D-glycero-β-D-arabino-hept-2-ulopyranose (First reaction of **Compound 3** in figure 28)

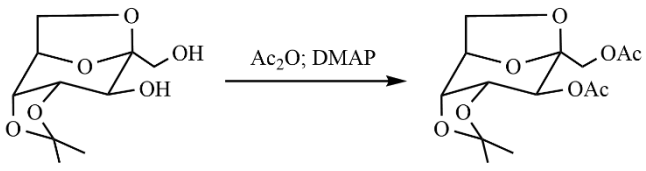

$C_{10}H_{16}O_6$
232.32 g/mol

$C_{14}H_{20}O_8$
316.31 g/mol

2,7-Anhydro-4,5-*O*-isopropylidene-D-glycero-β-D-arabino-hept-2-ulopyranose (514.3 mg, 2.22 mmol, 1 equiv.) was dissolved in dry pyridine (4.43 mL) under an argon atmosphere and

cooled to 0°C with an ice bath. Acetic anhydride (0.905 g, 0.85 mL, 8.86 mmol, 4 equiv.) was added dropwise followed by 4-(dimethylamino)pyridine (13.5 mg, 0.11 mmol, 0.05 equiv.). The ice bath was removed, and the solution was stirred at room temperature for 2 h. The reaction mixture was co-evaporated three times with toluene and the residue was dissolved in EA. The organic phase was washed twice with water and once with brine and dried with $MgSO_4$. It was filtered and evaporated to yield 1,3-Di-*O*-acetyl-2,7-anhydro-4,5-*O*-isopropylidene-D-glycero-β-D-arabino-hept-2-ulopyranose as a white solid which was used for the next reaction without further purification (582.9 mg, 83%); R_f = 0.31 (*n*-heptane/EA 2:1, CAM); ^{1}H NMR (700 MHz, $CDCl_3$) δ = 5.13 (d, $^3J_{3,4}$ = 5.66 Hz, 1H, H-3), 4.89 (d, $^3J_{6,7a}$ = 5.01 Hz, 1H, H-6), 4.39 (d, $^2J_{1a,1b}$ = 12.12 Hz, 1H, H-1a), 4.27 (t, $^3J_{4,3}$ = 6.02 Hz, $^3J_{4,5}$ = 5.79 Hz, 1H, H-4), 4.22 (dd, $^3J_{5,4}$ = 6.10 Hz, $^3J_{5,6}$ = 1.45 Hz, 1H, H-5), 3.96 (d, $^2J_{1b,1a}$ = 12.22 Hz, 1H, H-1b), 3.94 (d, $^2J_{7b,7a}$ = 5.01 Hz, 1H, H-7b), 3.90 (dd, $^2J_{7a,7b}$ = 7.83 Hz, $^3J_{7a,6}$ = 6.85 Hz, 1H, H-7a), 2.11 (s, 3H, $CH_3^{Ac\text{-}3}$), 2.08 (s, 3H, $CH_3^{Ac\text{-}1}$), 1.59 (s, 3H, $CH_3^{isopropylidene}$), 1.37 (s, 3H, $CH_3^{isopropylidene}$).

1,3-Di-*O*-acetyl-2,7-anhydro-D-glycero-β-D-arabino-hept-2-ulopyranose (Compound 3)

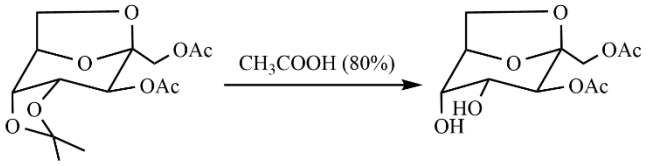

$C_{14}H_{20}O_8$
316.31 g/mol

$C_{11}H_{16}O_8$
276.24 g/mol

1,3-Di-*O*-acetyl-2,7-anhydro-4,5-*O*-isopropylidene-D-glycero-β-D-arabino-hept-2-ulopyranose (582.9 mg, 1.84 mmol, 1 equiv.) was dissolved in glacial acetic acid (11.52 mL) and water (2.92 mL) was added. The reaction mixture was stirred at 80°C for 2 h and after cooling to room temperature it was co-evaporated three times with toluene. The crude residue was recrystallized from ethanol yielding 1,3-di-*O*-acetyl-2,7-anhydro-D-glycero-β-D-arabino-hept-2-ulopyranose as a white solid (480.9 mg, 95%); R_f = 0.27 (EA, CAM); ^{1}H NMR (700 MHz, $CDCl_3$) δ = 4.97 (d, $^3J_{3,4}$ = 8.38 Hz, 1H, H-3), 4.77 (dd, $^3J_{6,7a}$ = 5.20 Hz, $^3J_{6,5}$ = 2.08 Hz, 1H, H-6), 4.53 (d, $^2J_{1a,1b}$ = 12.09 Hz, 1H, H-1a), 4.00 (d, $^2J_{1b,1a}$ = 12.02 Hz, 1H, H-1b), 3.96 (m, 1H, H-5), 3.93 (m, 1H, H-7a), 3.88 (dd, $^3J_{4,3}$ = 8.46 Hz, $^3J_{4,5}$ = 4.65 Hz, 1H, H-4), 3.84 (d, $^2J_{7b,7a}$ = 8.06 Hz, 1H, H-7b), 3.26 (s, 1H, OH-4), 2.80 (s, 1H, OH-5), 2.15 (s, 3H, $CH_3^{Ac\text{-}3}$), 2.09 (s, 3H, $CH_3^{Ac\text{-}1}$).

1,3-Di-*O*-acetyl-2,7-anhydro-4,5-*O*-benzylidene-D-glycero-β-D-arabino-hept-2-ulopyranose (**Compound 4)**

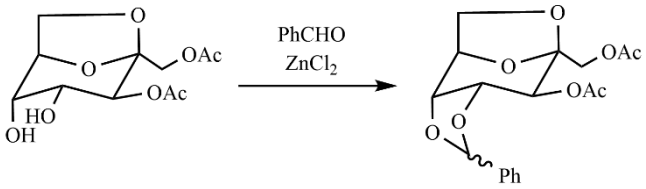

$C_{11}H_{16}O_8$
276.24 g/mol

$C_{18}H_{20}O_8$
364.35 g/mol

1,3-Di-*O*-acetyl-2,7-anhydro-D-glycero-β-D-arabino-hept-2-ulopyranose (480.9 mg, 1.74 mmol, 1 equiv.) was dissolved in benzaldehyde (3.48 mL) under an argon atmosphere. Zinc chloride (284.7 mg, 2.09 mmol, 1.2 equiv.) was melted with a Bunsen burner until no more evaporation of water could be observed, grinded in a mortar and added to the reaction mixture. The reaction mixture was stirred at room temperature for 4 h, afterwards diluted with DCM and washed with water and brine. The organic layer was dried ($MgSO_4$), filtered and evaporated. Remaining benzaldehyde was removed under reduced pressure at 80 °C for 4 h on a rotary evaporator to yield 1,3-di-*O*-acetyl-2,7-anhydro-4,5-*O*-benzylidene-D-glycero-β-D-arabino-hept-2-ulopyranose as a 1:1 mixture of exo- and endo-stereoisomers as a yellow oil, which was used for the next step without further purification (615.7 mg, 97%); Exo: R_f = 0.17 (*n*-heptane/EA 2:1, UV & CAM). ^{1}H NMR (700 MHz, $CDCl_3$) δ = 7.62 (m, 1H, H^{Ar}), 7.50-7.44 (m, 2H, H^{Ar}), 7.42-7.37 (m, 2H, H^{Ar}), 6.23 (s, 1H, H^{Bn}), 5.30 (d, $^3J_{3,4}$ = 5.84 Hz, 1H, H-3), 4.96 (d, $^3J_{6,7a}$ = 4.60 Hz, 1H, H-6), 4.60 (t, $^3J_{4,3}$ = $^3J_{4,5}$ = 6.05 Hz, 1H, H-4), 4.46 (d, $^2J_{1a,1b}$ = 12.23 Hz, 1H, H-1a), 4.25 (dd, $^3J_{5,4}$ = 6.01 Hz, $^3J_{5,6}$ = 1.22 Hz, 1H, H-5), 4.03 (d, $^2J_{1b,1a}$ = 3.78 Hz, 1H, H-1b), 3.95-3.90 (m, 2H, H-7a, H-7b), 2.15 (s, 3H, CH_3^{Ac-3}), 2.12 (s, 3H, CH_3^{Ac-1}). Endo: R_f = 0.25 (*n*-heptane/EA 2:1, UV & CAM). ^{1}H NMR (700 MHz, $CDCl_3$) δ = 7.65-7.60 (m, 1H, H^{Ar}), 7.59-7.55 (m, 2H, H^{Ar}), 7.50-7.45 (m, 2H, H^{Ar}), 5.93 (s, 1H, H^{Bn}), 5.19 (d, $^3J_{3,4}$ = 5.11 Hz, 1H, H-3), 5.03-5.00 (m, 1H, H-6), 4.41 (dd, $^3J_{4,5}$ = 6.74 Hz, $^3J_{4,3}$ = 4.89 Hz, 1H, H-4), 4.39 (d, $^2J_{1a,1b}$ = 12.05 Hz, 1H, H-1a), 4.30 (dd, $^3J_{5,4}$ = 6.74 Hz, $^3J_{5,6}$ = 0.91 Hz, 1H, H-5), 4.01 (d, $^2J_{1b,1a}$ = 12.16 Hz, 1H, H-1b), 3.94-3.90 (m, 2H, H-7a, H-7b), 2.12 (s, 3H, CH_3^{Ac-3}), 2.07 (s, 3H, CH_3^{Ac-1}).

1,3-Di-*O*-acetyl-2,7-anhydro-5-*O*-benzoyl-D-glycero-β-D-arabino-hept-2-ulopyranose (**Compound 5)**

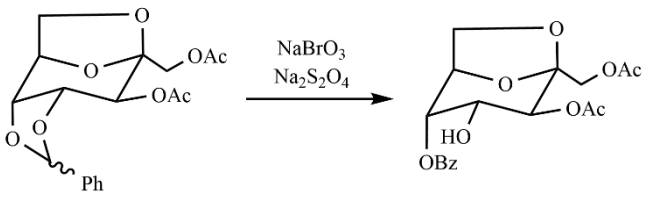

$C_{18}H_{20}O_8$
364.35 g/mol

$C_{18}H_{20}O_9$
380.35 g/mol

1,3-Di-*O*-acetyl-2,7-anhydro-4,5-*O*-benzylidene-D-glycero-β-D-arabino-hept-2-ulopyranose (615.7 mg, 1.68 mmol, 1 equiv.) was dissolved in EA (22.5 mL). Then sodium bromate (764.9 mg, 5.07 mmol, 3 equiv.) dissolved in water (11.3 mL) was added. Afterwards sodium dithionite (85% purity, 0.865 mg, 4.22 mmol, 2.5 equiv.) dissolved in water (22.5 mL) was added dropwise over the course of 10 minutes to the biphasic system. The reaction mixture was stirred at room temperature for 40 minutes and afterwards diluted with EA. The layers were separated and the aqueous was extracted three times with EA. The combined organic layers were washed with sat. aq. $Na_2S_2O_3$-solution, water and brine, dried over $MgSO_4$, filtered and evaporated. The crude residue was recrystallized from methanol and dried under reduced pressure yielding 1,3-di-*O*-acetyl-2,7-anhydro-5-*O*-benzoyl-D-glycero-β-D-arabino-hept-2-ulopyranose as a yellow-white foam (592 mg, 92%); R_f = 0.17 (*n*-heptane/EA 1:1, UV & CAM). ^{1}H NMR (700 MHz, $CDCl_3$) δ = 8.11 (d, $^3J_{H,H}$ = 8.55 Hz, 2H, H^{Ar}), 7.63 (t, $^3J_{H,H}$ = 7.29 Hz, 1H, H^{Ar}), 7.50 (t, $^3J_{H,H}$ = 7.75 Hz, 2H, H^{Ar}), 5.35 (dd, $^3J_{5,4}$ = 4.85 Hz, $^3J_{5,6}$ = 2.32 Hz, 1H, H-6), 5.22 (d, $^3J_{3,4}$ = 9.03 Hz, 1H, H-3), 4.93 (dd, $^3J_{6,7a}$ = 5.72 Hz, $^3J_{6,5}$ = 2.89 Hz, 1H, H-6), 4.56 (d, $^2J_{1a,1b}$ = 12.24 Hz, 1H, H-1a), 4.15 (m, 1H, H-4), 4.05 (d, $^3J_{1b,1a}$ = 12.17 Hz, 1H, H-1a), 3.96 (d, $^3J_{7a,7b}$ = 3.15 Hz, 2H, H-7a, H-7b), 2.23 (s, 1H, OH), 2.17 (s, 3H, $CH_3^{Ac\text{-}3}$), 2.11 (s, 3H, $CH_3^{Ac\text{-}1}$).

1,3-Di-*O*-acetyl-2,7-anhydro-5-*O*-benzoyl-4-*O*-trifluoromethanesulfonyl-D-glycero-β-D-arabino-hept-2-ulopyranose (**Compound 6)**

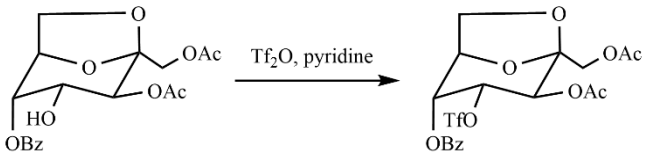

$C_{18}H_{20}O_9$
380.35 g/mol

$C_{19}H_{19}F_3O_{11}S$
512.41 g/mol

1,3-Di-*O*-acetyl-2,7-anhydro-5-*O*-benzoyl-D-glycero-β-D-arabino-hept-2-ulopyranose (592 mg, 1.55 mmol, 1 equiv.) was dissolved in dry DCM (7.78 mL) and cooled to 0°C. To this

solution pyridine (1.05 g, 1.07 mL, 13.23 mmol, 8.5 equiv.) and trifluoromethanesulfonic anhydride (0.88 g, 0.52 mL, 3.11 mmol, 2 equiv.) were added dropwise. The resulting mixture was stirred at 0°C for 1 h, diluted with 12 mL DCM and quenched by the dropwise addition of ice-cold 1M aq. HCl (8 mL). The layers were separated, and the aqueous layer was extracted twice with DCM. The combined organic layers were washed with ice-cold water, ice-cold aq. $NaHCO_3$-solution and ice-cold brine, dried ($MgSO_4$), filtered and evaporated. The crude residue was dried under vacuum to yield 1,3-di-*O*-acetyl-2,7-anhydro-5-*O*-benzoyl-4-*O*-trifluoromethanesulfonyl-D-glycero-β-D-arabino-hept-2-ulopyranose as a yellow foam. The product was used without any further purification. (746 mg, 94%); R_f = 0.72 (*n*-heptane/EA 1:1, UV & CAM). ^{1}H NMR (700 MHz, $CDCl_3$) δ = 8.10 (d, $^3J_{H,H}$ = 8.76 Hz, 2H, H^{Ar}), 7.64 (t, $^3J_{H,H}$ = 7.55 Hz, 1H, H^{Ar}), 7.51 (t, $^3J_{H,H}$ = 7.85 Hz, 2H, H^{Ar}), 5.58 (d, $^3J_{3,4}$ = 8.78 Hz, 1H, H-3), 5.58 (dd, $^3J_{5,4}$ = 5.28 Hz, $^3J_{5,6}$ = 2.46 Hz, 1H, H-5), 5.18 (dd, $^3J_{4,3}$ = 9.07 Hz, $^3J_{4,5}$ = 4.88 Hz, 1H, H-4), 5.00 (dd, $^3J_{6,7b}$ = 4.61 Hz, $^3J_{6,5}$ = 1.91 Hz, 1H, H-6), 4.56 (d, $^2J_{1a,1b}$ = 12.28 Hz, 1H, H-1a), 4.05-3.97 (m, 3H, H-7a, H-7b, H-1b), 2.15 (s, 3H, CH_3^{Ac-3}), 2.11 (s, 3H, CH_3^{Ac-1}).

1,4-Di-*O*-acetyl-2,7-anhydro-5-*O*-benzoyl-D-glycero-β-D-lyxo-hept-2-ulopyranose (**Compound 7a**) and 1,3-di-*O*-acetyl-2,7-anhydro-5-*O*-benzoyl-D-glycero-β-D-lyxo-hept-2-ulopyranose (**Compound 7b**)

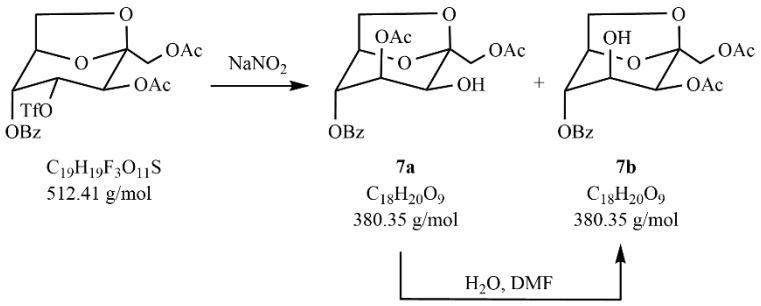

Crude 1,3-di-*O*-acetyl-2,7-anhydro-5-*O*-benzoyl-4-*O*-trifluoromethanesulfonyl-D-glycero-β-D-arabino-hept-2-ulopyranose (746 mg, 1.46 mmol, 1 equiv.) was dissolved in dry DMF (14.6 mL) under an argon atmosphere and sodium nitrite (1.00 g, 14.56 mmol, 10 equiv.) was added. The reaction mixture was stirred at 40°C for 80 h, diluted with EA and washed twice with water. The combined aqueous phases were extracted three times. The combined organic layers were washed with brine, dried ($MgSO_4$), filtered and evaporated. The crude residue was purified by column chromatography (70 g silica gel, n-heptane/EA 1:1). Since no sufficient separation was achieved the residue was further purified by MPLC (25 g silica gel, 15-60 % EA in toluene) yielding 1,3-di-*O*-acetyl-2,7-anhydro-5-*O*-benzoyl-D-glycero-β-D-lyxo-hept-2-ulopyranose **7b** (84.7 mg, 15%) and 1,4-di-*O*-acetyl-2,7-anhydro-5-*O*-benzoyl-D-glycero-β-D-lyxo-hept-2-

ulopyranose **7a** (132.6 mg, 24%) as a yellow-white foam each; **7a:** R_f = 0.23 (*n*-heptane/EA 1:1, UV & CAM). ^{1}H NMR (700 MHz, $CDCl_3$) δ = 8.07 (d, $^3J_{H,H}$ = 8.46 Hz, 2H, H^{Ar}), 7.61 (t, $^3J_{H,H}$ = 7.38 Hz, 1H, H^{Ar}), 7.47 (t, $^3J_{H,H}$ = 7.81 Hz, 2H, H^{Ar}), 5.37 (dt, $^3J_{4,3}$ = 5.96 Hz $^3J_{4,5}$ = $^3J_{4,6}$ = 1.71 Hz, 1H, H-4), 5.06 (t, $^3J_{5,4}$ = $^3J_{5,6}$ = 1.71 Hz, 1H, H-5), 4.79 (d, $^3J_{6,7b}$ = 5.03 Hz, 1H, H-6), 4.49 (d, $^2J_{1a,1b}$ = 12.13 Hz, 1H, H-1a), 4.34 (d, $^2J_{1b,1a}$ = 12.13 Hz, 1H, H-1b), 4.21 (dd, $^2J_{7a,7b}$ = 7.85 Hz, $^3J_{7a,6}$ = 0.62 Hz, 1H, H-7a), 4.11 (dd, $^3J_{4,OH}$ = 14.21 Hz, $^3J_{3,4}$ = 7.21 Hz, 1H, H-3), 3.96 (dd, $^2J_{7b,7a}$ = 7.55 Hz, $^3J_{7b,6}$ = 6.12 Hz, 1H, H-7b), 2.44 (d, $^3J_{OH,3}$ = 10.40 Hz, 1H, OH), 2.19 (s, 3H, $CH_3^{Ac\text{-}4}$), 2.15 (s, 3H, $CH_3^{Ac\text{-}1}$).

7b: R_f = 0.28 (*n*-heptane/EA 1:1, UV & CAM). ^{1}H NMR (700 MHz, $CDCl_3$) δ = 8.08 (d, $^3J_{H,H}$ = 8.35 Hz), 7.61 (t, $^3J_{H,H}$ = 7.38 Hz, 1H, H^{Ar}), 7.47 (t, $^3J_{H,H}$ = 7.78 Hz, 2H, H^{Ar}), 5.22 (t, $^3J_{5,4}$ = $^3J_{5,6}$ = 1.75 Hz, 1H, H-5), 5.17 (d, $^3J_{3,4}$ = 5.24 Hz, 1H, H-3), 4.85 (d, $^3J_{6,7b}$ = 5.20 Hz, 1H, H-6), 4.54 (d, $^2J_{1a,1b}$ = 12.08 Hz, 1H, H-1a), 4.44 (d, $^2J_{7a,7b}$ = 7.74 Hz, 1H, H-7a), 4.33 (m, 1H, H-4), 4.08 (d, $^2J_{1b,1a}$ = 12.16 Hz, 1H, H-1b), 3.95 (dd, $^2J_{7b,7a}$ = 7.55 Hz, $^3J_{7b,6}$ = 5.88 Hz, 1H, H-7b), 2.74 (d, $^3J_{OH,4}$ = 5.06 Hz, 1H, OH), 2.18 (s, 3H, $CH_3^{Ac\text{-}3}$), 2.11 (s, 3H, $CH_3^{Ac\text{-}1}$).

1,3-Di-*O*-acetyl-2,7-anhydro-5-*O*-benzoyl-4-*O*-trifluoromethanesulfonyl-D-glycero-β-D-lyxo-hept-2-ulopyranose (**Compound 8**)

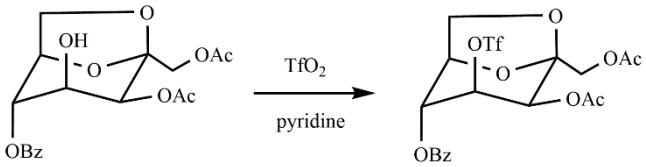

$C_{18}H_{20}O_9$
380.35 g/mol

$C_{19}H_{19}F_3O_{11}S$
512.41 g/mol

1,3-Di-*O*-acetyl-2,7-anhydro-5-*O*-benzoyl-D-glycero-β-D-lyxo-hept-2-ulopyranose (84.7 mg, 0.22 mmol, 1 equiv.) was dissolved in dry DCM (0.56 mL) and cooled to 0°C with an ice bath. To this solution pyridine (0.150 g, 0.152 mL, 1.89 mmol, 8.5 equiv.) and trifluoromethanesulfonic anhydride (0.126 mg, 0.075 mL, 0.45 mmol, 2 equiv.) were added dropwise over the course of 10 minutes. The resulting mixture was stirred at 0°C for 1 h, diluted with DCM (1.0 mL) and quenched by the dropwise addition of 1M HCl (0.75 mL). The layers were separated, and the aqueous layer was extracted twice with DCM. The combined organic layers were washed with ice-cold water, ice-cold aq. $NaHCO_3$-solution and ice-cold brine, dried ($MgSO_4$), filtered and evaporated. The crude residue was dried under vacuum to yield 1,3-di-*O*-acetyl-2,7-anhydro-5-*O*-benzoyl-4-*O*-trifluoromethanesulfonyl-D-glycero-β-D-lyxo-hept-2-ulopyranose as a yellow foam. The product was used without any further purification. (98.2 mg, 86%); Analytical data are identical as described for compound **6**.

Test synthesis for fluorination of compound 8 with KF/Kryptofix 2.2.2

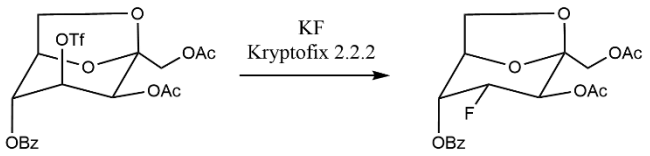

$C_{19}H_{19}F_3O_{11}S$
512.41 g/mol

$C_{18}H_{19}FO_8$
382.11 g/mol

1,3-Di-*O*-acetyl-2,7-anhydro-5-*O*-benzoyl-4-*O*-trifluoromethanesulfonyl-D-glycero-β-D-lyxo-hept-2-ulopyranose (49.1 mg, 0.096 mmol, 1 equiv.) was dissolved in dry acetonitrile (0.25 mL) in a dry flask. Potassium fluoride (11.1 mg, 0.192 mmol, 2 equiv.) and Kryptofix 222 (72.2 mg, 0.192 mmol, 2 equiv.) were dried under an argon atmosphere for 10 minutes. Kryptofix was then dissolved in 0.75 mL dry ACN and added to dry KF. The resulting solution was the added to compound **8** and the mixture was heated to 50 °C for 1.5 h. After 1.5 h a small sample (0.1 mL) was taken, and the solvent was removed on a rotary evaporator. Then a TLC (n-heptane/EA 1:1) was performed and a ^{1}H-NMR spectrum was recorded. The reaction mixture was then stepwise heated to 70°C, 90°C and finally 110°C for 1.5 h each and analysed as described above.

Test synthesis for fluorination of compound 8 with tetrabutylammonium fluoride trihydrate

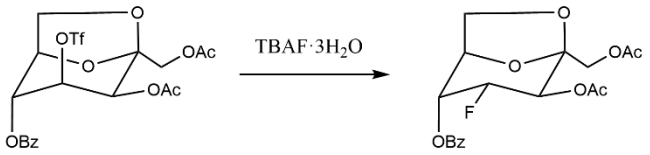

$C_{19}H_{19}F_3O_{11}S$
512.41 g/mol

$C_{18}H_{19}FO_8$
382.11 g/mol

In a dry flask 1,3-di-*O*-acetyl-2,7-anhydro-5-*O*-benzoyl-4-*O*-trifluoromethanesulfonyl-D-glycero-β-D-lyxo-hept-2-ulopyranose (49.1 mg, 0.096 mmol, 1 equiv.) was dissolved in dry acetonitrile (0.5 mL). Tetrabutylammonium fluoride trihydrate (120.9 mg, 0.383 mmol, 4 equiv.) was dried under high vacuum and elevated temperature for 10 minutes and then dissolved in dry acetonitrile (0.5 mL). The reaction flask was heated to 70°C and tetrabutylammonium fluoride trihydrate was added dropwise which caused a colour change from orange to brown. After 1.5 h a small sample (0.1 mL) was taken. The sample was quenched with 0.1 mL water, extracted three times with DCM, dried ($MgSO_4$) and the solvent was removed on a rotary evaporator. Then a TLC (n-heptane/EA 1:1) was performed and a ^{1}H-NMR spectrum was recorded.; this procedure was repeated after 1.5 h at 70, 90 and finally 110 °C each.

References

(1) Champagne, P. A.; Desroches, J.; Hamel, J.-D.; Vandamme, M.; Paquin, J.-F. Monofluorination of Organic Compounds: 10 Years of Innovation. *Chemical reviews* **2015**, *115*, 9073–9174.

(2) Furuya, T.; Kuttruff, C. A.; Ritter, T. Carbon-fluorine bond formation. *Current opinion in drug discovery & development* **2008**, *11*, 803–819.

(3) Card, P. J. Synthesis of Fluorinated Carbohydrates. *Journal of Carbohydrate Chemistry* **1985**, *4*, 451–487.

(4) Uhrig, M. L.; Lantaño, B.; Postigo, A. Synthetic strategies for fluorination of carbohydrates. *Organic & biomolecular chemistry* **2019**, *17*, 5173–5189.

(5) Hevey, R. The Role of Fluorine in Glycomimetic Drug Design. *Chemistry (Weinheim an der Bergstrasse, Germany)* **2021**, *27*, 2240–2253.

(6) O'Hagan, D. Understanding organofluorine chemistry. An introduction to the C-F bond. *Chemical Society reviews* **2008**, *37*, 308–319.

(7) Jacobson, O.; Kiesewetter, D. O.; Chen, X. Fluorine-18 radiochemistry, labeling strategies and synthetic routes. *Bioconjugate chemistry* **2015**, *26*, 1–18.

(8) Wang, Y.; Lin, Q.; Shi, H.; Cheng, D. Fluorine-18: Radiochemistry and Target-Specific PET Molecular Probes Design. *Frontiers in chemistry* **2022**, *10*, 884517.

(9) Fowler, J. S.; Ido, T. Initial and subsequent approach for the synthesis of 18FDG. *Seminars in nuclear medicine* **2002**, *32*, 6–12.

(10) Littich, R.; Scott, P. J. H. Neue Strategien für die 18 F-Radiochemie. *Angewandte Chemie* **2012**, *124*, 1132–1135.

(11) Beuthien-Baumann, B.; Hamacher, K.; Oberdorfer, F.; Steinbach, J. Preparation of fluorine-18 labelled sugars and derivatives and their application as tracer for positron-emission-tomography. *Carbohydrate research* **2000**, *327*, 107–118.

(12) Adam, M. J. A rapid, stereoselective, high yielding synthesis of 2-deoxy-2-fluoro-D-hexopyranoses: reaction of glycals with acetyl hypofluorite. *J. Chem. Soc., Chem. Commun.* **1982**, 730.

(13) Yu, S. Review of F-FDG Synthesis and Quality Control. *Biomedical imaging and intervention journal* **2006**, *2*, e57.

(14) Koziorowski, J. A simple method for the quality control of (18)FFDG. *Applied radiation and isotopes : including data, instrumentation and methods for use in agriculture, industry and medicine* **2010**, *68*, 1740–1742.

(15) Currie, G. M.; Wheat, J. M.; Davidson, R.; Kiat, H. Radionuclide production. *Radiographer* **2011**, *58*, 46–52.
(16) Pichler, V.; Berroterán-Infante, N.; Philippe, C.; Vraka, C.; Klebermass, E.-M.; Balber, T.; Pfaff, S.; Nics, L.; Mitterhauser, M.; Wadsak, W. An Overview of PET Radiochemistry, Part 1: The Covalent Labels 18F, 11C, and 13N. *Journal of nuclear medicine : official publication, Society of Nuclear Medicine* **2018**, *59*, 1350–1354.
(17) Miller, P. W.; Long, N. J.; Vilar, R.; Gee, A. D. Synthesis of 11C, 18F, 15O, and 13N radiolabels for positron emission tomography. *Angewandte Chemie (International ed. in English)* **2008**, *47*, 8998–9033.
(18) Cole, E. L.; Stewart, M. N.; Littich, R.; Hoareau, R.; Scott, P. J. H. Radiosyntheses using fluorine-18: the art and science of late stage fluorination. *Current topics in medicinal chemistry* **2014**, *14*, 875–900.
(19) Campbell, E.; Jordan, C.; Gilmour, R. Fluorinated carbohydrates for 18F-positron emission tomography (PET). *Chemical Society reviews* **2023**, *52*, 3599–3626.
(20) Wernick, M. N.; Aarsvold, J. N. *Emission Tomography*; Elsevier Science, 2004.
(21) Adam, M. J. Radiohalogenated carbohydrates for use in PET and SPECT. *Labelled Comp Radiopharmac* **2002**, *45*, 167–180.
(22) Zhang, X.; Basuli, F.; Shi, Z.-D.; Shah, S.; Shi, J.; Mitchell, A.; Lai, J.; Wang, Z.; Hammoud, D. A.; Swenson, R. E. Synthesis and Evaluation of Fluorine-18-Labeled L-Rhamnose Derivatives. *Molecules (Basel, Switzerland)* **2023**, *28*.
(23) Namavari, M.; Gowrishankar, G.; Hoehne, A.; Jouannot, E.; Gambhir, S. S. Synthesis of ^{18}F-labelled maltose derivatives as PET tracers for imaging bacterial infection. *Molecular imaging and biology* **2015**, *17*, 168–176.
(24) Haradahira, T.; Kato, A.; Maeda, M.; Torii, Y.; Ichiya, Y.; Masuda, K. Synthesis and biodistribution of a fluorine-18 labeled analogue of D-talose: 2-deoxy-2-18Ffluoro-D-talose. *International journal of radiation applications and instrumentation. Part A, Applied radiation and isotopes* **1992**, *43*, 627–632.
(25) Onega, M.; Domarkas, J.; Deng, H.; Schweiger, L. F.; Smith, T. A. D.; Welch, A. E.; Plisson, C.; Gee, A. D.; O'Hagan, D. An enzymatic route to 5-deoxy-5-18Ffluoro-D-ribose, a 18F-fluorinated sugar for PET imaging. *Chemical communications (Cambridge, England)* **2010**, *46*, 139–141.
(26) Kohlmeier, M. Carbohydrates. *Nutrient Metabolism*; Elsevier, 2003; pp 187–193.
(27) Huonnic, K.; Linclau, B. The Synthesis and Glycoside Formation of Polyfluorinated Carbohydrates. *Chemical reviews* **2022**, *122*, 15503–15602.

(28) Dong, H.; Pei, Z.; Ramström, O. Stereospecific ester activation in nitrite-mediated carbohydrate epimerization. *The Journal of organic chemistry* **2006**, *71*, 3306–3309.
(29) Chandel, N. S. Carbohydrate Metabolism. *Cold Spring Harbor perspectives in biology* **2021**, *13*.
(30) Doores, K. J.; Gamblin, D. P.; Davis, B. G. Exploring and exploiting the therapeutic potential of glycoconjugates. *Chemistry (Weinheim an der Bergstrasse, Germany)* **2006**, *12*, 656–665.
(31) Kannagi, R. Regulatory roles of carbohydrate ligands for selectins in the homing of lymphocytes. *Current opinion in structural biology* **2002**, *12*, 599–608.
(32) Berg, J. M.; Tymoczko, J. L.; Gatto, G. J.; Stryer, L. *Stryer Biochemie*; Springer Berlin Heidelberg: Berlin, Heidelberg, 2018.
(33) Tang, M.; Etokidem, E.; Lai, K. The Leloir Pathway of Galactose Metabolism - A Novel Therapeutic Target for Hepatocellular Carcinoma. *Anticancer research* **2016**, *36*, 6265–6271.
(34) Laughlin, M. R. Normal roles for dietary fructose in carbohydrate metabolism. *Nutrients* **2014**, *6*, 3117–3129.
(35) Patra, K. C.; Hay, N. The pentose phosphate pathway and cancer. *Trends in biochemical sciences* **2014**, *39*, 347–354.
(36) Stincone, A.; Prigione, A.; Cramer, T.; Wamelink, M. M. C.; Campbell, K.; Cheung, E.; Olin-Sandoval, V.; Grüning, N.-M.; Krüger, A.; Tauqeer Alam, M.*; et al.* The return of metabolism: biochemistry and physiology of the pentose phosphate pathway. *Biological reviews of the Cambridge Philosophical Society* **2015**, *90*, 927–963.
(37) Dringen, R.; Hoepken, H. H.; Minich, T.; Ruedig, C. 1.3 Pentose Phosphate Pathway and NADPH Metabolism. In *Handbook of Neurochemistry and Molecular Neurobiology*; Lajtha, A., Gibson, G. E., Dienel, G. A., Eds.; Springer US: Boston, MA, 2007; pp 41–62.
(38) Kruger, N. J.; Schaewen, A. von. The oxidative pentose phosphate pathway: structure and organisation. *Current opinion in plant biology* **2003**, *6*, 236–246.
(39) TeSlaa, T.; Ralser, M.; Fan, J.; Rabinowitz, J. D. The pentose phosphate pathway in health and disease. *Nature metabolism* **2023**, *5*, 1275–1289.
(40) Jiang, P.; Du, W.; Wu, M. Regulation of the pentose phosphate pathway in cancer. *Protein & cell* **2014**, *5*, 592–602.
(41) Nagy, C.; Haschemi, A. Sedoheptulose kinase regulates cellular carbohydrate metabolism by sedoheptulose 7-phosphate supply. *Biochemical Society transactions* **2013**, *41*, 674–680.
(42) Tauseef Ahmad Khan; Amna Ahmed; John Sievenpiper. *Rare sugars*, 2022.

(43) Haschemi, A.; Kosma, P.; Gille, L.; Evans, C. R.; Burant, C. F.; Starkl, P.; Knapp, B.; Haas, R.; Schmid, J. A.; Jandl, C.*; et al.* The sedoheptulose kinase CARKL directs macrophage polarization through control of glucose metabolism. *Cell metabolism* **2012**, *15*, 813–826.

(44) Gallagher, B. M.; Fowler, J. S.; Gutterson, N. I.; MacGregor, R. R.; Wan, C. N.; Wolf, A. P. Metabolic trapping as a principle of oradiopharmaceutical design: some factors resposible for the biodistribution of 18F 2-deoxy-2-fluoro-D-glucose. *Journal of nuclear medicine : official publication, Society of Nuclear Medicine* **1978**, *19*, 1154–1161.

(45) Larson, S. M. Gallagher's Principle of Metabolic Trapping. *Journal of nuclear medicine : official publication, Society of Nuclear Medicine* **2020**, *61*, 74S-76S.

(46) Scheibelberger, L.; Stankovic, T.; Pühringer, M.; Kählig, H.; Balber, T.; Patronas, E.-M.; Rampler, E.; Mitterhauser, M.; Haschemi, A.; Pallitsch, K. Synthesis of 4-Deoxy-4-Fluoro-d-Sedoheptulose: A Promising New Sugar to Apply the Principle of Metabolic Trapping. *Chemistry (Weinheim an der Bergstrasse, Germany)* **2023**, *29*, e202302277.

(47) Adinolfi, M.; Barone, G.; Guariniello, L.; Iadonisi, A. Facile cleavage of carbohydrate benzyl ethers and benzylidene acetals using the reagent under two-phase conditions. *Tetrahedron Letters* **1999**, *40*, 8439–8441.

(48) Kim, D. W.; Jeong, H.-J.; Lim, S. T.; Sohn, M.-H. Tetrabutylammonium Tetra(tert -Butyl Alcohol)-Coordinated Fluoride as a Facile Fluoride Source. *Angewandte Chemie* **2008**, *120*, 8532–8534.